Tech Briefs

NATIONAL AERONAUTICS AND SPACE ADMINISTRATION

- **Technology Focus**

- **Electronics/Computers**

- **Software**

- **Materials**

- **Mechanics**

- **Machinery/Automation**

- **Manufacturing**

- **Bio-Medical**

- **Physical Sciences**

- **Information Sciences**

- **Books and Reports**

INTRODUCTION

Tech Briefs are short announcements of innovations originating from research and development activities of the National Aeronautics and Space Administration. They emphasize information considered likely to be transferable across industrial, regional, or disciplinary lines and are issued to encourage commercial application.

Availability of NASA Tech Briefs and TSPs

Requests for individual Tech Briefs or for Technical Support Packages (TSPs) announced herein should be addressed to

National Technology Transfer Center

Telephone No. **(800) 678-6882** or via World Wide Web at **www2.nttc.edu/leads/**

Please reference the control numbers appearing at the end of each Tech Brief. Information on NASA's Commercial Technology Team, its documents, and services is also available at the same facility or on the World Wide Web at **www.nctn.hq.nasa.gov**.

Commercial Technology Offices and Patent Counsels are located at NASA field centers to provide technology-transfer access to industrial users. Inquiries can be made by contacting NASA field centers and program offices listed below.

NASA Field Centers and Program Offices

Ames Research Center
Carolina Blake
(650) 604-1754
carolina.m.blake@nasa.gov

Dryden Flight Research Center
Jenny Baer-Riedhart
(661) 276-3689
jenny.baer-riedhart@dfrc.nasa.gov

Goddard Space Flight Center
Nona Cheeks
(301) 286-5810
Nona.K.Cheeks.1@gsfc.nasa.gov

Jet Propulsion Laboratory
Art Murphy, Jr.
(818) 354-3480
arthur.j.murphy-jr@jpl.nasa.gov

Johnson Space Center
Charlene E. Gilbert
(281) 483-3809
commercialization@jsc.nasa.gov

Kennedy Space Center
Jim Aliberti
(321) 867-6224
Jim.Aliberti-1@ksc.nasa.gov

Langley Research Center
Jesse Midgett
(757) 864-3936
jesse.c.midgett@nasa.gov

John H. Glenn Research Center at Lewis Field
Larry Viterna
(216) 433-3484
cto@grc.nasa.gov

Marshall Space Flight Center
Vernotto McMillan
(256) 544-2615
vernotto.mcmillan@msfc.nasa.gov

Stennis Space Center
Robert Bruce
(228) 688-1929
robert.c.bruce@nasa.gov

NASA Program Offices

At NASA Headquarters there are seven major program offices that develop and oversee technology projects of potential interest to industry:

Carl Ray
Small Business Innovation Research Program (SBIR) & Small Business Technology Transfer Program (STTR)
(202) 358-4652 or
cray@mail.hq.nasa.gov

Benjamin Neumann
InnovativeTechnology Transfer Partnerships (Code RP)
(202) 358-2320
benjamin.j.neumann@nasa.gov

John Mankins
Office of Space Flight (Code MP)
(202) 358-4659 or
jmankins@mail.hq.nasa.gov

Terry Hertz
Office of Aero-Space Technology (Code RS)
(202) 358-4636 or
thertz@mail.hq.nasa.gov

Glen Mucklow
Office of Space Sciences (Code SM)
(202) 358-2235 or
gmucklow@mail.hq.nasa.gov

Roger Crouch
Office of Microgravity Science Applications (Code U)
(202) 358-0689 or
rcrouch@hq.nasa.gov

Granville Paules
Office of Mission to Planet Earth (Code Y)
(202) 358-0706 or
gpaules@mtpe.hq.nasa.gov

TECH BRIEFS

NATIONAL AERONAUTICS AND SPACE ADMINISTRATION

Technology Focus: Test & Measurement

COTS MEMS Flow-Measurement Probes

These relatively inexpensive probes are compact and have short response times.

John H. Glenn Research Center, Cleveland, Ohio

As an alternative to conventional tubing instrumentation for measuring airflow, designers and technicians at Glenn Research Center have been fabricating packaging components and assembling a set of unique probes that contain commercial off-the-shelf (COTS) microelectromechanical systems (MEMS) sensor chips. MEMS sensor chips offer some compelling advantages over standard macroscopic measurement devices. MEMS sensor technology has matured through mass production and use in the automotive and aircraft industries. At present, MEMS are the devices of choice for sensors in such applications as tire-pressure monitors, altimeters, pneumatic controls, cable leak detectors, and consumer appliances. Compactness, minimality of power demand, rugged construction, and moderate cost all contribute to making MEMS sensors attractive for instrumentation for future research.

Conventional macroscopic flow-measurement instrumentation includes tubes buried beneath the aerodynamic surfaces of wind-tunnel models or in wind-tunnel walls. Pressure is introduced at the opening of each such tube. The pressure must then travel along the tube before reaching a transducer that generates an electronic signal. The lengths of such tubes typically range from 20 ft (≈ 6 m) to hundreds of feet (of the order of 100 m). The propagation of pressure signals in the tubes damps the signals con-
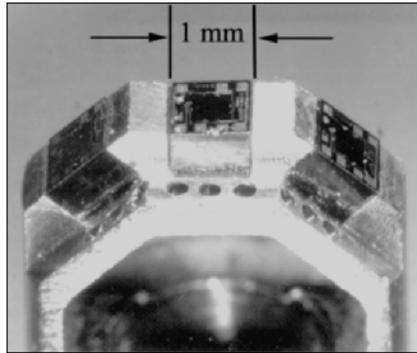
This **Probe Containing Three COTS MEMS Sensor Chips** is designed to measure flow angularity in a plane. A planned similar probe will contain five MEMS sensors for measuring flow angularity in three dimensions.

siderably and makes it necessary to delay measurements until after test rigs have reached steady-state operation. In contrast, a MEMS pressure sensor that generates electronic output can take readings continuously under dynamic conditions in nearly real time.

In order to use stainless-steel tubing for pressure measurements, it is necessary to clean many tubes, cut them to length, carefully install them, delicately deburr them, and splice them. A cluster of a few hundred 1/16-in.- (≈1.6-mm-) diameter tubes (such clusters are common in research testing facilities) can be several inches (of the order of 10 cm) in diameter and could weigh enough that two technicians are needed to handle it. Replacing hard tubing with electronic

chips can eliminate much of the bulk. Each sensor would fit on the tip of a 1/16-in. tube with room to spare.

The Lucas NovaSensor P592 piezoresistive silicon pressure sensor was chosen for this project because of its cost, availability, and tolerance to extreme ambient conditions. The sensor chip is 1 mm square by 0.6 mm thick (about 0.039 by 0.039 by 0.024 in.) and includes 0.12-mm (≈0.005-in.) wire connection tabs.

The figure shows a flow-angularity probe that was built by use of three such MEMS chips. It is planned to demonstrate this MEMS probe as an alternative to a standard tube-type "Cobra" probe now used routinely in wind tunnels and aeronautical hardware. This MEMS probe could be translated across a flow field by use of a suitable actuator, so that its accuracy and the shortness of its response time could be exploited to obtain precise dynamic measurements of a sort that cannot be made by use of conventional tubing-based instrumentation.

Measurement of an Evaporating Drop on a Reflective Substrate

This system complements a prior one for measuring on a transparent substrate.

John H. Glenn Research Center, Cleveland, Ohio

The figure depicts an apparatus that simultaneously records magnified ordinary top-view video images and laser-shadowgraph video images of a sessile drop on a flat, horizontal substrate that can be opaque or translucent and is at least partially specularly reflective. A similar apparatus for recording such images

of a drop on a transparent substrate was described in "Measuring Contact Angles of a Sessile Drop and Imaging Convection Within It" (LEW-17075), *NASA Tech Briefs*, Vol. 25, No. 3 (March 2001), page 50. As in the case of the previously reported apparatus, the diameter, contact angle, and rate of evaporation of the

drop as functions of time can be calculated from the apparent diameters of the drop in sequences of the images acquired at known time intervals, and the shadowgrams that contain flow patterns indicative of thermocapillary convection (if any) within the drop. These time-dependent parameters and flow patterns
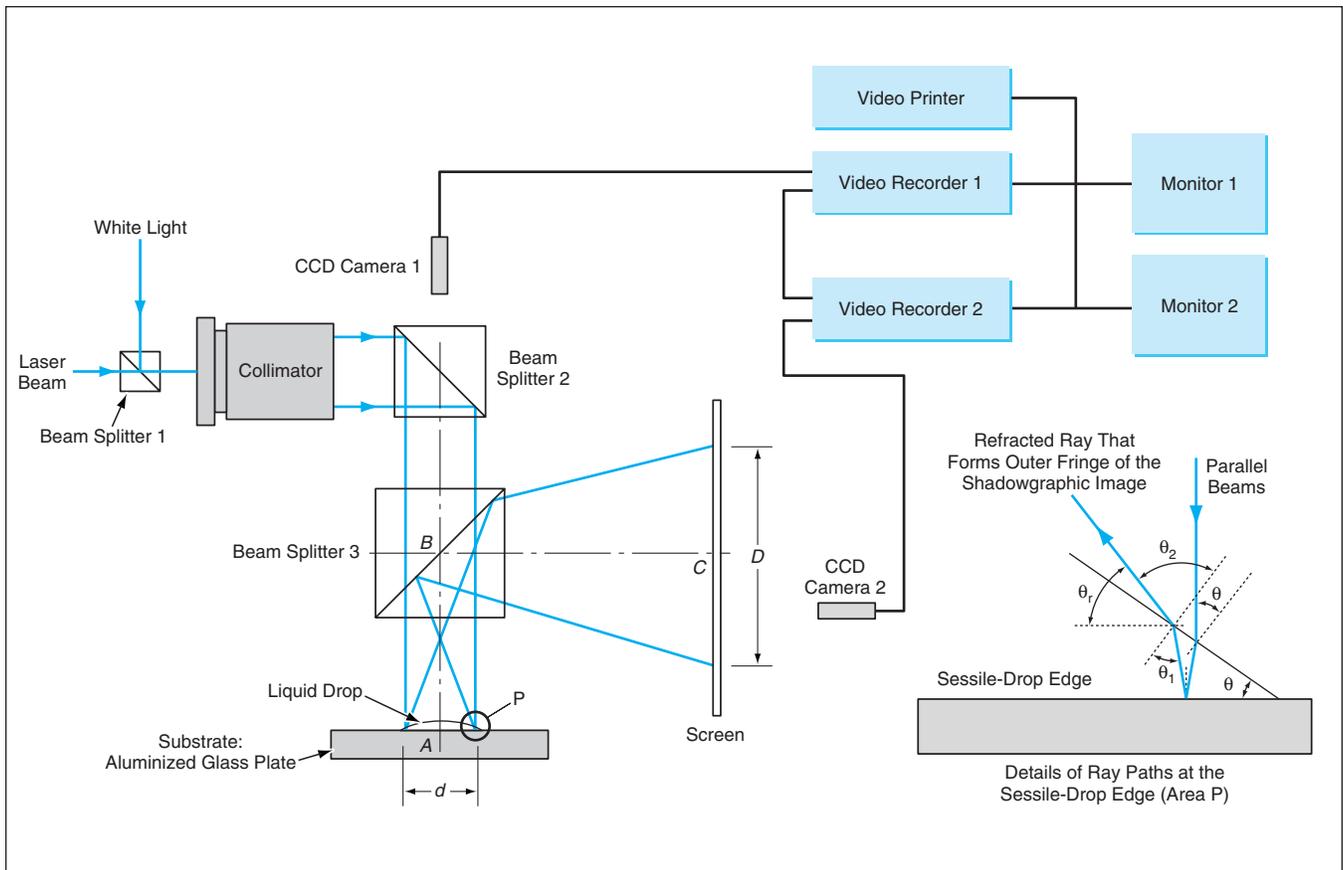
The **Time-Dependent Diameters _d_ and _D_** measured in images acquired by cameras 1 and 2 can be used to calculate the contact angle, volume, and other parameters of the drop on the substrate at point A.

are important for understanding the physical processes involved in the spreading and evaporation of drops.

The apparatus includes a source of white light and a laser (both omitted from the figure), which are used to form the ordinary image and the shadowgram, respectively. Charge-coupled-device (CCD) camera 1 (with zoom) acquires the ordinary video images, while CCD camera 2 acquires the shadowgrams. With respect to the portion of laser light specularly reflected from the substrate, the drop acts as a plano-convex lens, focusing the laser beam to a shadowgram on the projection screen in front of CCD camera 2.

The equations for calculating the diameter, contact angle, and rate of evaporation of the drop are readily derived on the basis of Snell's law of refraction and the geometry of the optics. The equations differ from those for the apparatus of the cited prior article. Omitting intermediate steps of the derivation for the sake of brevity, the results are the following:

The two related unknown quantities are the contact angle (θ) and, for light that has been reflected from the substrate, the angle of refraction (θ_2) of that light from

the surface of the drop at a point near edge. These quantities are found by solving the simultaneous equations

$$\frac{2s}{(d+D)} = \frac{\cot\theta_2 + \tan\theta}{1 - \cot\theta_2 \tan\theta}$$

and

$$\sin\theta_2 = n\sin 2\theta\sqrt{1 - \frac{\sin^2\theta}{n^2}} - \cos 2\theta \sin\theta,$$

where n is the index of refraction of the liquid in the drop, s = the total length of paths AB and BC, d is the apparent diameter of the drop as measured in the ordinary image acquired by CCD camera 1, and D is the diameter of the shadowgraphic image acquired by CCD camera 2.

On the basis of a spherical-cap approximation of the shape of the drop, the thickness of the drop (h) at its apex is given by

$$h = \frac{d(1 - \cos\theta)}{2\sin\theta}$$

and the volume (Ω) of the drop is given by

$$\Omega = \pi h^2\left(\frac{d}{2\sin\theta} - \frac{h}{3}\right).$$

The time-average rate of evaporation of the drop, W_{av}, is considered to be an important parameter for quantifying evaporation strength and can be determined by

$$W_{av} = \frac{\Omega_0}{t_f},$$

where Ω_0 is the initial volume of the drop and t_f is the lifetime of the drop. The instantaneous rate of evaporation can be calculated by

$$W = \frac{\Delta\Omega}{\Delta t},$$

where $\Delta\Omega$ is the difference between the volumes of the drop at two measurement times separated by the interval Δt.

# Airplane Ice Detector Based on a Microwave Transmission Line

Electrical measurements are affected by thawing, freezing, and the presence or absence of water.

Lyndon B. Johnson Space Center, Houston, Texas

An electronic instrument that could detect the potentially dangerous buildup of ice on an airplane wing is undergoing development. The instrument is based on a microwave transmission line configured as a capacitance probe: at selected spots, the transmission-line conductors are partly exposed to allow any ice and/or liquid water present at those spots to act as predominantly capacitive electrical loads on the transmission line. These loads change the input impedance of the transmission line, as measured at a suitable excitation frequency. Thus, it should be possible to infer the presence of ice and/or liquid water from measurements of the input impedance and/or electrical parameters related to the input impedance.

The sensory transmission line is of the microstrip type and thus thin enough to be placed on an airplane wing without unduly disturbing airflow in flight. The sensory spots are small areas from which the upper layer of the microstrip has been removed to allow any liquid water or ice on the surface to reach the transmission line. The sensory spots are spaced at nominal open-circuit points, which are at intervals of a half wavelength (in the transmission line, not in air) at the excitation frequency. The excitation frequency used in the experiments has been 1 GHz, for which a half wavelength in the transmission line is ≈4 in. (≈10 cm).

The figure depicts a laboratory prototype of the instrument. The impedance-related quantities chosen for use in this version of the instrument are the magnitude and phase of the scattering parameter S_{11} as manifested in the in-phase (I) and quadrature (Q) outputs of the phase detector. By careful layout of the transmission line (including the half-wavelength sensor spacing), one can ensure that the amplitude and phase of the input to the phase detector keep shifting
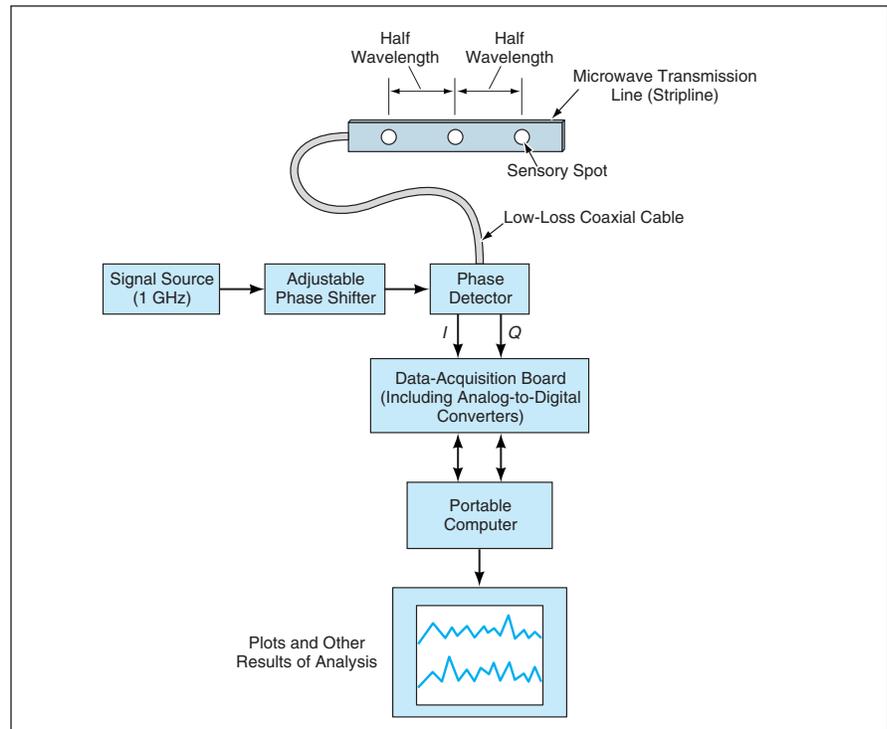
The ***I* and *Q* Outputs of the Phase Shifter** are affected by the presence or absence of liquid water or ice on the sensory spots on the microwave transmission line.

in the same direction as ice forms on one or more of the sensor areas. Although only one transmission-line sensor strip is used in the laboratory version, in a practical application, it could be desirable to install multiple strips on different areas to detect localized icing. In that case, a multiplexer should be used to connect the various strips to the phase detector for sequential measurements.

Experiments have been performed with freezing and thawing of water and of water/glycol mixtures. The experiments have shown that, whether or not glycol is present, it is possible to distinguish between liquid water and ice via the I and Q outputs; in particular, the equipment can

be adjusted so that when water freezes, I decreases and Q increases. With respect to the operation of this instrument, the main effect of glycol is to increase the freezing or thawing time.

This work was done by G. Dickey Arndt and Phong Ngo of **Johnson Space Center** *and James R. Carl of Lockheed Martin. For further information, contact G. Dickey Arndt at g.d.arndt@nasa.gov.*

This invention is owned by NASA, and a patent application has been filed. Inquiries concerning nonexclusive or exclusive license for its commercial development should be addressed to the Patent Counsel, Johnson Space Center, (281) 483-0837. Refer to MSC-23118.

Microwave/Sonic Apparatus Measures Flow and Density in Pipe

The entire flow, rather than a small diverted sample flow, is probed.

Lyndon B. Johnson Space Center, Houston, Texas

An apparatus for measuring the rate of flow and the mass density of a liquid or slurry includes a special section of pipe instrumented with microwave and sonic

sensors, and a computer that processes digitized readings taken by the sensors. The apparatus was conceived specifically for monitoring a flow of oil-well-drilling

mud, but the basic principles of its design and operation are also applicable to monitoring flows of other liquids and slurries.

In one configuration, a special section

The **Height of the Fluid** relative to the antenna is determined from differences between the phases of stepped-frequency microwave signals transmitted to, and reflected from, the top surface of the fluid.

Fourier transform to compute the round-trip propagation time of the signal reflected from top of the fluid. The height of the fluid is then computed from the round-trip travel time and the known height of the antenna. A sonic sensor that operates alongside the microwave sensor gives an approximate height reading that makes it possible to resolve the integer-multiple-of-2π phase ambiguity of the microwave sensor, while the microwave sensor makes it possible to refine the height measurement to within 0.1 in. ($\approx$2.5 mm).

Ultrasonic sensors on the walls near the bottom of the special section of pipe are used to measure the speed of sound needed to compute the density of the fluid. More specifically, what is measured is the difference between the phase of a signal of known frequency at a transmitting transducer and the phase of the same signal at a receiving transducer a known distance away. It may also be necessary to resolve an integer-multiple-of-2π phase ambiguity. This can be done by using two sonic frequencies chosen according to a well-established technique. Alternatively, one could use a single sonic frequency low enough not to be subject to the phase ambiguity, albeit with some loss of density resolution. Simulations indicate that a density accuracy measurement of 0.25 percent (0.0025) can be attained with a single-tone system.

This work was done by G. D. Arndt and Phong Ngo of **Johnson Space Center** *and J. R. Carl and Kent A. Byerly, independent consultants.*

This invention is owned by NASA, and a patent application has been filed. Inquiries concerning nonexclusive or exclusive license for its commercial development should be addressed to the Patent Counsel, Johnson Space Center, (281) 483-0837. Refer to MSC-23311.

of pipe is located immediately upstream of the point of discharge of the flow to be monitored. The special section of pipe must be large enough that the pipe can accommodate the entire flow of interest (in contradistinction to a small diverted sample flow), that the flow remains laminar at all times, and that the pipe is never entirely full, even at the maximum flow rate.

In another configuration, the apparatus does not measure the rate of flow or the density directly: Instead, it (a) measures the height of the fluid in the special section of pipe and computes the flow rate as a predetermined function of the height and (b) measures the speed of sound in the fluid and computes the density of the fluid as a predetermined function of the speed of sound in the fluid. To enable the apparatus to per-

form these computations, one must calibrate the apparatus, prior to operation, by measuring the flow rate as a function of height and the mass density as a function of the speed of sound for the drilling mud or other fluid of interest.

In the second configuration, the velocity of the fluid can be measured subsurface using a set of one transmitter and two receivers to measure differential phase shifts. This second configuration can be used within a filled or unfilled closed pipe to measure volume flow. The microwave portion of the apparatus (see figure) includes a broadband swept-frequency (more precisely, stepped-frequency) transmitter/receiver pair connected, via a directional coupler, to an antenna aimed downward at the liquid. Transmitted- and received-signal data are processed by an algorithm that uses a modified

---

Reducing Errors by Use of Redundancy in Gravity Measurements

Mathematical identities are exploited to suppress noise or reduce numbers of measurements.

NASA's Jet Propulsion Laboratory, Pasadena, California

A methodology for improving gravity-gradient measurement data exploits the constraints imposed upon the components of the gravity-gradient tensor by the conditions of integrability needed for reconstruction of the gravitational potential. These constraints are derived

from the basic equation for the gravitational potential and from mathematical identities that apply to the gravitational potential and its partial derivatives with respect to spatial coordinates.

Consider the gravitational potential ϕ in a Cartesian coordinate system $\{x_1, x_2, x_3\}$.

The ith component of gravitational acceleration is given by

$$g_i = -\frac{\partial \phi}{\partial x_i}$$

(where i = 1, 2, or 3) and the (α, β) com-

ponent of the gravity-gradient tensor is given by

$$\Gamma_{\alpha\beta} \equiv \frac{-\partial g_\alpha}{\partial x_\beta} = \frac{\partial^2 \phi}{\partial x_\beta \partial x_\alpha}$$

where α = 1, 2, or 3 and β = 1, 2, or 3. The aforementioned constraints are such that the components of the gravity-gradient tensor are not independent of each other. In particular, it is easily shown that the gravity-gradient tensor is symmetrical and has a zero trace; that is,

$\Gamma_{\alpha\beta} = \Gamma_{\beta\alpha}$ and $\Gamma_{11} + \Gamma_{22} + \Gamma_{33} = 0$. Hence, if one measures all the components of the gravity-gradient tensor at all points of interest within a region of space in which one seeks to characterize the gravitational field, one obtains redundant information. One could utilize the constraints to select a minimum (that is, nonredundant) set of measurements from which the gravitational potential could be reconstructed. Alternatively, one could exploit the redundancy to reduce errors from noisy measurements.

A convenient example is that of the selection of a minimum set of measurements to characterize the gravitational field at n^3 points (where n is an integer) in a cube. Without the benefit of such a selection, it would be necessary to make $9n^3$ measurements because the gravity-gradient tensor has 9 components at each point. It has been shown that when the constraints are applied to the measurement points in an appropriately chosen sequence, the number of measurements needed to compute all $9n^3$ components is only $n^3 + n^2 + 3n$.

The problem of utilizing the redundancy to reduce errors in noisy measurements is an optimization problem: Given a set of noisy values of the components of the gravity-gradient tensor at the measurement points, one seeks a set of corrected values — a set that is optimum in that it minimizes some measure of error (e.g., the sum of squares of the differences between the corrected and noisy measurement values) while taking account of the fact that the constraints must apply to the exact values. The problem as thus posed leads to a vector equation that can be solved to obtain the corrected values.

Membrane-Based Water Evaporator for a Space Suit

This design incorporates recent advances in hydrophobic micropore membranes.

Lyndon B. Johnson Space Center, Houston, Texas

A membrane-based water evaporator has been developed that is intended to serve as a heat-rejection device for a space suit. This evaporator would replace the current sublimator that is sensitive to contamination of its feedwater. The design of the membrane-based evaporator takes advantage of recent advances in hydrophobic micropore membranes to provide robust heat rejection with much less sensitivity to contamination. The low contamination sensitivity allows use of the heat transport loop as feedwater, eliminating the need for the separate feedwater system used for the sublimator.

A cross section of the evaporator is shown in the accompanying figure. The space-suit cooling loop water flows into a distribution plenum, through a narrow annulus lined on both sides with a hydrophobic membrane, into an exit plenum, and returns to the space suit. Two perforated metal tubes encase the membranes and provide structural strength. Evaporation at the membrane inner surface dissipates the waste heat from the space suit. The water vapor passes through the membrane, into a steam duct and is vented to the vacuum environment through a back-pressure
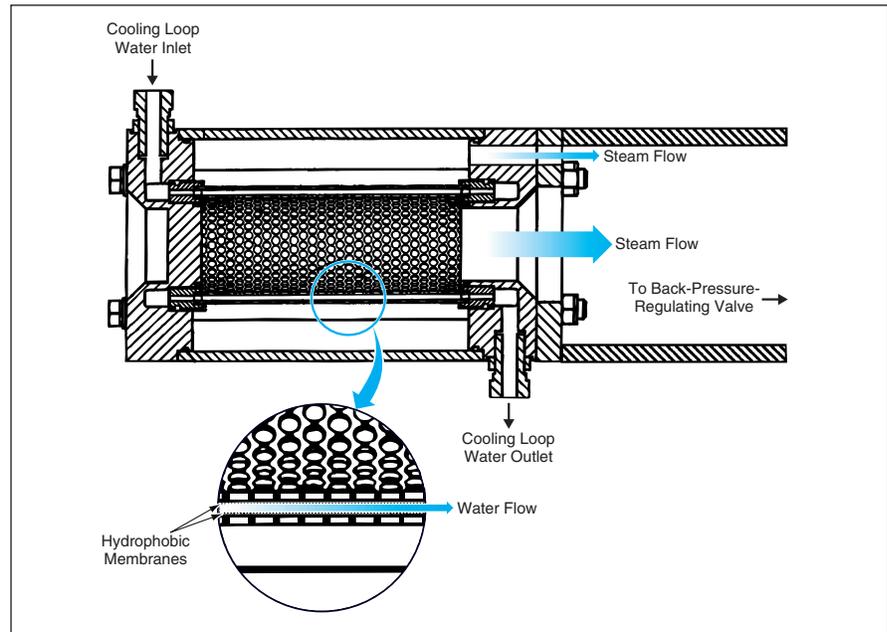
Hydrophobic Membranes provide the basis for a simple, robust device for space-suit heat rejection.

valve. The back-pressure setting can be adjusted to regulate the heat-rejection rate and the water outlet temperature.

This work was done by Eugene K. Ungar and Charles J. McCann of **Johnson Space Center** *and Mary K. O'Connell and Scott Andrea of Lockheed Martin Corp. For further information, contact the Johnson Commercial Technology Office at (281) 483-3809. MSC-23317*

Compact Microscope Imaging System With Intelligent Controls

This system automates tasks that, heretofore, required the full attention of human technicians.

John H. Glenn Research Center, Cleveland, Ohio

The figure presents selected views of a compact microscope imaging system (CMIS) that includes a miniature video microscope, a Cartesian robot (a computer-controlled three-dimensional translation stage), and machine-vision and control subsystems. The CMIS was built from commercial off-the-shelf instrumentation, computer hardware and software, and custom machine-vision software. The machine-vision and control subsystems include adaptive neural networks that afford a measure of artificial intelligence.

The CMIS can perform several automated tasks with accuracy and repeata-

bility — tasks that, heretofore, have required the full attention of human technicians using relatively bulky conventional microscopes. In addition, the automation and control capabilities of the system inherently include a capability for remote control. Unlike human technicians, the CMIS is not at risk of becoming fatigued or distracted: theoretically, it can perform continuously at the level of the best human technicians. In its capabilities for remote control and for relieving human technicians of tedious routine tasks, the CMIS is expected to be especially useful in bio-

medical research, materials science, inspection of parts on industrial production lines, and space science.

The CMIS can automatically focus on and scan a microscope sample, find areas of interest, record the resulting images, and analyze images from multiple samples simultaneously. Automatic focusing is an iterative process: The translation stage is used to move the microscope along its optical axis in a succession of coarse, medium, and fine steps. A fast Fourier transform (FFT) of the image is computed at each step, and the FFT is analyzed for its spatial-fre-
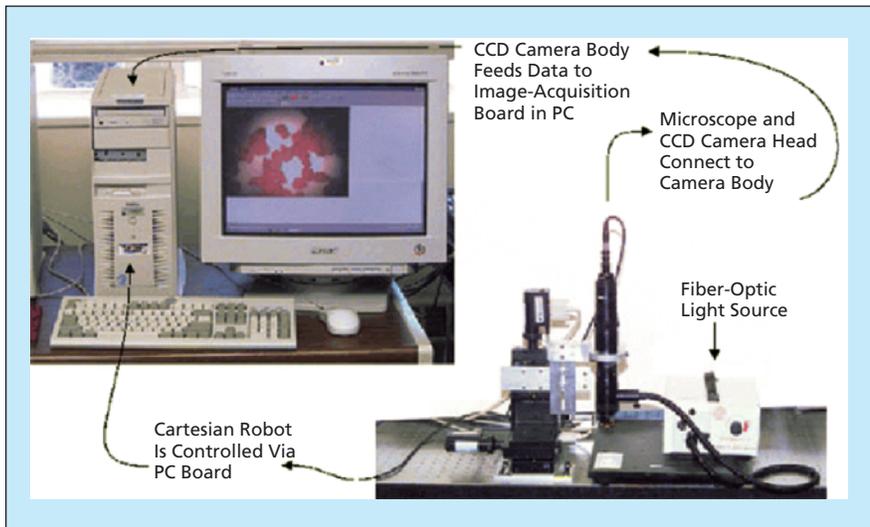
The **CMIS Takes Less Room** than does a conventional microscope. Unlike a conventional microscope, the CMIS offers capabilities for remote control and for automation of routine tasks.

- *Identification and Classification of Objects*: The system can find, classify, and label objects [e.g., living cells of one or more type(s) of interest] within a predetermined area of interest.
- *Motion Detection*: Movements of objects in a predetermined area of interest can be observed and quantified.
- *Transition Mapping*: In a sample containing small particles (e.g., colloids or living cells), small transitions between groups of particles can be detected. Examples of transitions include those between order and disorder, large and small objects, light and dark regions, and movement and non-movement. For example, in the case of a colloidal suspension containing a liquid and an adjacent solid phase, this function can be helpful in locating the zone of transition between the two phases.

This work was done by Mark McDowell of **Glenn Research Center**. *Further information is contained in a TSP (see page 1).*

Inquiries concerning rights for the commercial use of this invention should be addressed to NASA Glenn Research Center, Commercial Technology Office, Attn: Steve Fedor, Mail Stop 4-8, 21000 Brookpark Road, Cleveland, Ohio 44135. Refer to LEW-17484.

quency content. The microscope position that results in the greatest dispersal of FFT content toward high spatial frequencies (indicating that the image shows the greatest amount of detail) is deemed to be the focal position.

In addition to automatic focusing, the machine-vision system is capable of performing the following other functions:

- *Adaptive Thresholding*: This function enables the choice of the best contrast needed for other image processing.
- *Auto-Imaging Scanning*: The microscope can scan along any or all of three Cartesian coordinate axes within a sample in order to find an object of interest.

Chirped-Superlattice, Blocked-Intersubband QWIP
Collection efficiency and, hence, quantum efficiency are expected to increase.

NASA's Jet Propulsion Laboratory, Pasadena, California

An $Al_xGa_{1-x}As/GaAs$ quantum-well infrared photodetector (QWIP) of the blocked-intersubband-detector (BID) type, now undergoing development, features a chirped (that is, aperiodic) superlattice. The purpose of the chirped superlattice is to increase the quantum efficiency of the device.

A somewhat lengthy background discussion is necessary to give meaning to a brief description of the present developmental QWIP. A BID QWIP was described in "MQW Based Block Intersubband Detector for Low-Background Operation" (NPO-21073), *NASA Tech Briefs* Vol. 25, No. 7 (July 2001), page 46. To recapitulate: The BID design was conceived in response to the deleterious effects of operation of a QWIP at low temperature under low background radiation. These effects can be summarized as a buildup of space charge and an associated high impedance and diminution of responsivity with increasing modulation frequency.

The BID design, which reduces these deleterious effects, calls for a heavily doped multiple-quantum-well (MQW) emitter section with barriers that are thinner than in prior MQW devices. The thinning of the barriers results in a large overlap of sublevel wave functions, thereby creating a miniband. Because of sequential resonant quantum-mechanical tunneling of electrons from the negative ohmic contact to and between wells, any space charge is quickly neutralized. At the same time, what would otherwise be a large component of dark current attributable to tunneling current through the whole device is suppressed by placing a relatively thick, undoped, impurity-free $Al_xGa_{1-x}As$ blocking barrier layer between the MQW emitter section and the positive ohmic contact. [This layer is similar to the thick, undoped $Al_xGa_{1-x}As$ layers used in photodetectors of the blocked-impurity-band (BIB) type.]

Notwithstanding the aforementioned advantage afforded by the BID design, the responsivity of a BID QWIP is very low because of low collection efficiency, which, in turn, is a result of low electrostatic-potential drop across the superlattice emitter. Because the emitter must be electrically conductive to prevent the buildup of space charge in depleted quantum wells, most of the externally applied bias voltage drop occurs across the blocking-barrier layer. This completes the background discussion.

In the developmental QWIP, the periodic superlattice of the prior BID design is to be replaced with the chirped superlattice, which is expected to provide a built-in electric field. As a result, the efficiency of collection of photoexcited charge carriers (and, hence, the net quantum efficiency and thus responsivity) should increase significantly.

This work was done by Sarath Gunapala, David Ting, and Sumith Bandara of Caltech for **NASA's Jet Propulsion Laboratory**. *Further information is contained in a TSP (see page 1).*
NPO-30510

Charge-Dissipative Electrical Cables

Lossy dielectric layers and grounding conductors drain spurious charges to ground.

Goddard Space Flight Center, Greenbelt, Maryland

Electrical cables that dissipate spurious static electric charges, in addition to performing their main functions of conducting signals, have been developed. These cables are intended for use in trapped-ion or ionizing-radiation environments, in which electric charges tend to accumulate within, and on the surfaces of, dielectric layers of cables. If the charging rate exceeds the dissipation rate, charges can accumulate in excessive amounts, giving rise to high-current discharges that can damage electronic circuitry and/or systems connected to it.

The basic idea of design and operation of charge-dissipative electrical cables is to drain spurious charges to ground by use of lossy (slightly electrically conductive) dielectric layers, possibly in conjunction with drain wires and/or drain shields (see figure). In typical cases, the drain wires and/or drain shields could be electrically grounded via the connector assemblies at the ends of the cables, in any of the conventional techniques for grounding signal conductors and signal shields. In some cases, signal shields could double as drain shields.

To be suitable for use in a charge-dissipating cable, a dielectric material must be inherently lossy throughout its bulk, and not, say, an insulating polymer with a conductive surface film or containing embedded conductive particles. Conductive surface films can be rendered inef-fective by flaking off or cracking, especially when cables are bent. Embedded particles can act as defect sites that initiate arcing within dielectric layers.

The concept of lossiness can be quantified: Dielectric materials can be broadly categorized, as either "excellent" or "lossy" according to their volume electrical resistivity (ρ) values. Excellent insulators may be roughly categorized as having ρ of the order of $10^{16}\Omega{\cdot}m$, while lossy or dissipative insulators may be categorized as having ρ of the order of $10^9\ \Omega{\cdot}m$.

In designing for a specific application, one must choose the lossy dielectric material and the configuration of grounding conductors to be capable of dissipating a sufficient proportion of static charge within an acceptably short time. For a typical cable that handles signals of sufficiently low frequencies (having wavelengths much greater than the length of the cable), the effective charge-dissipating admittance or conductance must be much less than the nominal signal admittance or signal conductance of the circuits connected with the cable, so as not to adversely affect the transmission of signals. For a typical cable that handles signals of sufficiently high frequencies (having wavelengths comparable to or less than the length of the cable), the effective charge-dissipating admittance or conductance must be taken into account as part of the overall signal-propagation cable imped-
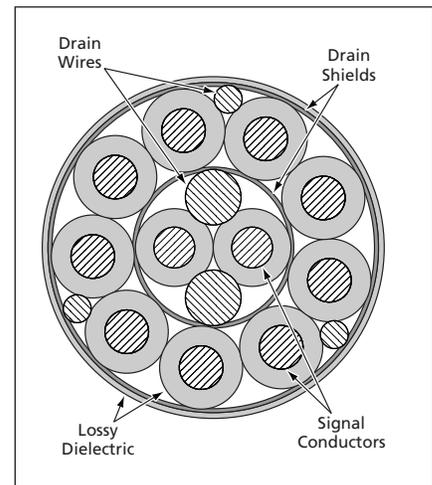
This **Cross Section** illustrates one of many possible charge-dissipating designs for a cable containing 11 signal conductors.

ance, and the signal attenuation caused by loss in the dielectric must be acceptably low. These requirements could be difficult to satisfy if a cable is too long and, hence, imposes either a limit on the allowable length of the cable or else a requirement to pay closer attention to interactions between the charge-dissipation and signal-propagation aspects of the cable design.

This work was done by John R. Kolasinski and Edward J. Wollack of **Goddard Space Flight Center**. *Further information is contained in a TSP (see page 1).*
GSC-14648-1

Deep-Sea Video Cameras Without Pressure Housings

Camera units could be made smaller, lighter, and less expensive.

NASA's Jet Propulsion Laboratory, Pasadena, California

Underwater video cameras of a proposed type (and, optionally, their light sources) would not be housed in pressure vessels. Conventional underwater cameras and their light sources are housed in pods that keep the contents dry and maintain interior pressures of about 1 atmosphere ($\approx$0.1 MPa). Pods strong enough to withstand the pressures at great ocean depths are bulky, heavy, and expensive. Elimination of the pods would make it possible to build camera/light-source units that would be significantly smaller, lighter, and less ex-pensive. The depth ratings of the proposed camera/light source units would be essentially unlimited because the strengths of their housings would no longer be an issue.

A camera according to the proposal would contain an active-pixel image sensor and readout circuits, all in the form of a single silicon-based complementary metal oxide/semiconductor (CMOS) integrated-circuit chip. As long as none of the circuitry and none of the electrical leads were exposed to seawater, which is electrically conductive, silicon inte-grated-circuit chips could withstand the hydrostatic pressure of even the deepest ocean. The pressure would change the semiconductor band gap by only a slight amount — not enough to degrade imaging performance significantly.

Electrical contact with seawater would be prevented by potting the integrated-circuit chip in a transparent plastic case. The electrical leads for supplying power to the chip and extracting the video signal would also be potted, though not necessarily in the same transparent plastic. The hydrostatic pressure would tend

to compress the plastic case and the chip equally on all sides; there would be no need for great strength because there would be no need to hold back high pressure on one side against low pressure on the other side. A light source suitable for use with the camera could consist of light-emitting diodes (LEDs). Like integrated-circuit chips, LEDs can withstand very large hydrostatic pressures.

If power-supply regulators or filter capacitors were needed, these could be attached in chip form directly onto the back of, and potted with, the imager chip. Because CMOS imagers dissipate little power, the potting would not result in overheating. To minimize the cost of the camera, a fixed lens could be fabricated as part of the plastic case. For improved optical performance at greater cost, an adjustable glass achromatic lens would be mounted in a reservoir that would be filled with transparent oil and subject to the full hydrostatic pressure, and the reservoir would be mounted on the case to position the lens in front of the image sensor. The lens would by adjusted for focus by use of a motor inside the reservoir (oil-filled motors already exist).

RFID and Memory Devices Fabricated Integrally on Substrates
These molecularly bonded devices would be much thinner than microchips.

Marshall Space Flight Center, Alabama

Electronic identification devices containing radio-frequency identification (RFID) circuits and antennas would be fabricated integrally with the objects to be identified, according to a proposal. That is to say, the objects to be identified would serve as substrates for the deposition and patterning of the materials of the devices used to identify them, and each identification device would be bonded to the identified object at the molecular level. Vacuum arc vapor deposition (VAVD) is the NASA–derived process for depositing layers of material on the substrate.

This proposal stands in contrast to the current practice of fabricating RFID and/or memory devices as wafer-based, self-contained integrated-circuit chips that are subsequently embedded in or attached to plastic cards to make "smart" account-information cards and identification badges. If one relies on such a chip to store data on the history of an object to be tracked and the chip falls off or out of the object, then one loses both the his-

torical data and the means to track the object and verify its identity electronically. Also, in contrast is the manufacturing philosophy in use today to make many memory devices. Today's methods involve many subtractive processes such as etching. This proposal only uses additive methods, building RFID and memory devices from the substrate up in thin layers. VAVD is capable of spraying silicon, copper, and other materials commonly used in electronic devices. The VAVD process sprays most metals and some ceramics. The material being sprayed has a very strong bond with the substrate, whether that substrate is metal, ceramic, or even wood, rock, glass, PVC, or paper.

An object to be tagged with an identification device according to the proposal must be compatible with a vacuum deposition process. Temperature is seldom an issue as the substrate rarely reaches 150° F (66° C) during the deposition process. A portion of the surface of the object would be designated as a substrate for the deposition of the device. By use of a vacuum arc vapor deposition apparatus, a thin electrically insulating film would first be deposited on the substrate. Subsequent layers of materials would then be deposited and patterned by use of known integrated-circuit fabrication techniques. The total thickness of the deposited layers could be much less than the 100-μm thickness of the thinnest state-of-the-art self-contained microchips. Such a thin deposit could be readily concealed by simply painting over it. Both large vacuum chambers for production runs and portable hand-held devices for *in situ* applications are available.

Software

Analyzing Dynamics of Cooperating Spacecraft

A software library has been developed to enable high-fidelity computational simulation of the dynamics of multiple spacecraft distributed over a region of outer space and acting with a common purpose. All of the modeling capabilities afforded by this software are available independently in other, separate software systems, but have not previously been brought together in a single system. A user can choose among several dynamical models, many high-fidelity environment models, and several numerical-integration schemes. The user can select whether to use models that assume weak coupling between spacecraft, or strong coupling in the case of feedback control or tethering of spacecraft to each other. For weak coupling, spacecraft orbits are propagated independently, and are synchronized in time by controlling the step size of the integration. For strong coupling, the orbits are integrated simultaneously. Among the integration schemes that the user can choose are Runge-Kutta Verner, Prince-Dormand, Adams-Bashforth-Moulton, and Bulirsh-Stoer. Comparisons of performance are included for both the weak- and strong-coupling dynamical models for all of the numerical integrators. The library was designed for ease of integration with high-fidelity environment models already in use in the Flight Dynamics Analysis Branch, which is one of seven institutional support branches within the Mission Engineering and Systems Analysis Division at Goddard Space Flight Center.

This program was written by Stephen P. Hughes and David C. Folta of **Goddard Space Flight Center** *and Darrel J. Conway of Thinking Systems, Inc. Further information is contained in a TSP (see page 1). GSC-14735-1*

Spacecraft Attitude Maneuver Planning Using Genetic Algorithms

A key enabling technology that leads to greater spacecraft autonomy is the capability to autonomously and optimally slew the spacecraft from and to different attitudes while operating under a number of celestial and dynamic constraints.

The task of finding an attitude trajectory that meets all the constraints is a formidable one, in particular for orbiting or fly-by spacecraft where the constraints and initial and final conditions are of time-varying nature. This approach for attitude path planning makes full use of *a priori* constraint knowledge and is computationally tractable enough to be executed onboard a spacecraft. The approach is based on incorporating the constraints into a cost function and using a Genetic Algorithm to iteratively search for and optimize the solution. This results in a directed random search that explores a large part of the solution space while maintaining the knowledge of good solutions from iteration to iteration. A solution obtained this way may be used 'as is' or as an initial solution to initialize additional deterministic optimization algorithms. A number of representative case examples for time-fixed and time-varying conditions yielded search times that are typically on the order of minutes, thus demonstrating the viability of this method. This approach is applicable to all deep space and planet Earth missions requiring greater spacecraft autonomy, and greatly facilitates navigation and science observation planning.

This work was done by Richard P. Kornfeld of Caltech for **NASA's Jet Propulsion Laboratory**. *Further information is contained in a TSP (see page 1).*

This software is available for commercial licensing. Please contact Don Hart of the California Institute of Technology at (818) 393-3425. Refer to NPO-40107.

Forensic Analysis of Compromised Computers

Directory Tree Analysis File Generator is a Practical Extraction and Reporting Language (PERL) script that simplifies and automates the collection of information for forensic analysis of compromised computer systems. During such an analysis, it is sometimes necessary to collect and analyze information about files on a specific directory tree. Directory Tree Analysis File Generator collects information of this type (except information about directories) and writes it to a text file. In particular, the script asks the user for the root of the directory tree to be processed, the name of the output file, and the number of subtree levels to process. The script then processes the directory tree and puts out the aforementioned text file. The format of the text file is designed to enable the submission of the file as input to a spreadsheet program, wherein the forensic analysis is performed. The analysis usually consists of sorting files and examination of such characteristics of files as ownership, time of creation, and time of most recent access, all of which characteristics are among the data included in the text file.

This program was written by Thomas Wolfe of Caltech for **NASA's Jet Propulsion Laboratory**. *Further information is contained in a TSP (see page 1).*

This software is available for commercial licensing. Please contact Don Hart of the California Institute of Technology at (818) 393-3425. Refer to NPO-40165.

Document Concurrence System

The Document Concurrence System is a combination of software modules for routing users expressions of concurrence with documents. This system enables determination of the current status of concurrences and eliminates the need for the prior practice of manually delivering paper documents to all persons whose approvals were required. This system runs on a server, and participants gain access via personal computers equipped with Web-browser and electronic-mail software. A user can begin a concurrence routing process by logging onto an administration module, naming the approvers and stating the sequence for routing among them, and attaching documents. The server then sends a message to the first person on the list. Upon concurrence by the first person, the system sends a message to the second person, and so forth. A person on the list indicates approval, places the documents on hold, or indicates disapproval, via a Web-based module. When the last person on the list has concurred, a message is sent to the initiator, who can then finalize the process through the administration module. A background process running on the server identifies concurrence processes that are overdue and sends reminders to the appropriate persons.

Σ Managing an Archive of Images

The SSC Multimedia Archive is an automated electronic system to manage images, acquired both by film and digital cameras, for the Public Affairs Office (PAO) at Stennis Space Center (SSC). Previously, the image archive was based on film photography and utilized a manual system that, by today's standards, had become inefficient and expensive. Now, the SSC Multimedia Archive, based on a server at SSC, contains both catalogs and images for pictures taken both digitally and with a traditional, film-based camera, along with metadata about each image. After a "shoot," a photographer downloads the images into the database. Members of the PAO can use a Web-based application to search, view and retrieve images, approve images for publication, and view and edit metadata associated with the images. Approved images are archived and cross-referenced with appropriate descriptions and information. Security is provided by allowing administrators to explicitly grant access privileges to personnel to only access components of the system that they need to (i.e., allow only photographers to upload images, only PAO designated employees may approve images).

☢ MPT Prediction of Aircraft-Engine Fan Noise

A collection of computer programs has been developed that implements a procedure for predicting multiple-pure-tone (MPT) noise generated by fan blades of an aircraft engine (e.g., a turbofan engine). MPT noise arises when the fan is operating with supersonic relative tip Mach No. Under this flow condition, there is a strong upstream running shock. The strength and position of this shock are very sensitive to blade geometry variations. For a fan where all the blades are identical, the primary tone observed upstream of the fan will be the blade passing frequency. If there are small variations in geometry between blades, then tones below the blade passing frequency arise — MPTs. Stagger angle differences as small as 0.1° can give rise to significant MPT. It is also noted that MPT noise is more pronounced when the fan is operating in an "unstarted" mode. Computational results using a three-dimensional flow solver to compute the complete annulus flow with non-uniform fans indicate that MPT noise can be estimated in a relatively simple way. Hence, once the effect of a typical geometry variation of one blade in an otherwise uniform blade row is known, the effect of all the blades being different can be quickly computed via superposition. Two computer programs that were developed as part of this work are used in conjunction with a user's computational fluid dynamics (CFD) code to predict MPT spectra for a fan with a specified set of geometric variations:

- The first program ROTBLD reads the users CFD solution files for a single blade passage via an API (Application Program Interface). There are options to replicate and perturb the geometry with typical variations stagger, camber, thickness, and pitch. The multi-passage CFD solution files are then written in the user's file format using the API.

- The second program SUPERPOSE requires two input files: the first is the circumferential upstream pressure distribution extracted from the CFD solution on the multi-passage mesh, the second file defines the geometry variations of each blade in a complete fan. Superposition is used to predict the spectra resulting from the geometric variations.

The user would typically generate a multi-passage mesh (ROTBLD) with the geometry of one blade perturbed — typically, four or five passages are required. A CFD solution would then be generated for this mesh. Using this solution and specified geometry variations for a complete fan, the MPT spectra can be estimated using SUPERPOSE.

☢ Improving Control of Two Motor Controllers

A computer program controls motors that drive translation stages in a metrology system that consists of a pair of two-axis cathetometers. This program is specific to Compumotor Gemini (or equivalent) motors and the Compumotor 6K-series (or equivalent) motor controller. Relative to the software supplied with the controller, this program affords more capabilities and is easier to use. Written as a Virtual Instrument in the LabVIEW software system, the program presents an imitation control panel that the user can manipulate by use of a keyboard and mouse. There are three modes of operation: command, movement, and joystick. In command mode, single commands are sent to the controller for troubleshooting. In movement mode, distance, speed, and/or acceleration commands are sent to the controller. Position readouts from the motors and from position encoders on the translation stages are displayed in marked fields. At any time, the position readouts can be recorded in a file named by the user. In joystick mode, the program yields control of the motors to a joystick. The program sends commands to, and receives data from, the controller via a serial cable connection, using the serial-communication portion of the software supplied with the controller.

# Electrodeionization Using Microseparated Bipolar Membranes

Low concentrations of ions do not inhibit further removal of ions.

Lyndon B. Johnson Space Center, Houston, Texas

An electrochemical technique for deionizing water, now under development, is intended to overcome a major limitation of prior electrically–based water-purification techniques. The limitation in question is caused by the desired decrease in the concentration of ions during purification: As the concentration of ions decreases, the electrical resistivity of the water increases, posing an electrical barrier to the removal of the remaining ions. In the present technique, this limitation is overcome by use of electrodes, a flow-field structure, and solid electrolytes configured to provide conductive paths for the removal of ions from the water to be deionized, even when the water has already been purified to a high degree.

The technique involves the use of a bipolar membrane unit (BMU), which includes a cation-exchange membrane and an anion-exchange membrane separated by a nonconductive mesh that has been coated by an ionically conductive material (see figure). The mesh ensures the desired microseparation between the ion-exchange membranes: The interstices bounded by the inner surfaces of the membranes and the outer surfaces of the coated mesh constitute a flow-field structure that allows the water that one seeks to deionize (hereafter called "process water" for short) to flow through the BMU with a low pressure drop. The flow-field structure is such that the distance between any point in the flow field and an ionically conductive material is small; thus, the flow-field structure facilitates the diffusion of molecules and ions to and from the ion-exchange membranes.

The BMU is placed between an anode and a cathode, but not in direct contact with these electrodes. Instead, the space between the anionexchange membrane and the anode is denoted the anode compartment and is filled with an ionic solution. Similarly, the space between the cation-exchange membrane and the cathode is denoted the cathode compartment and is filled with a different
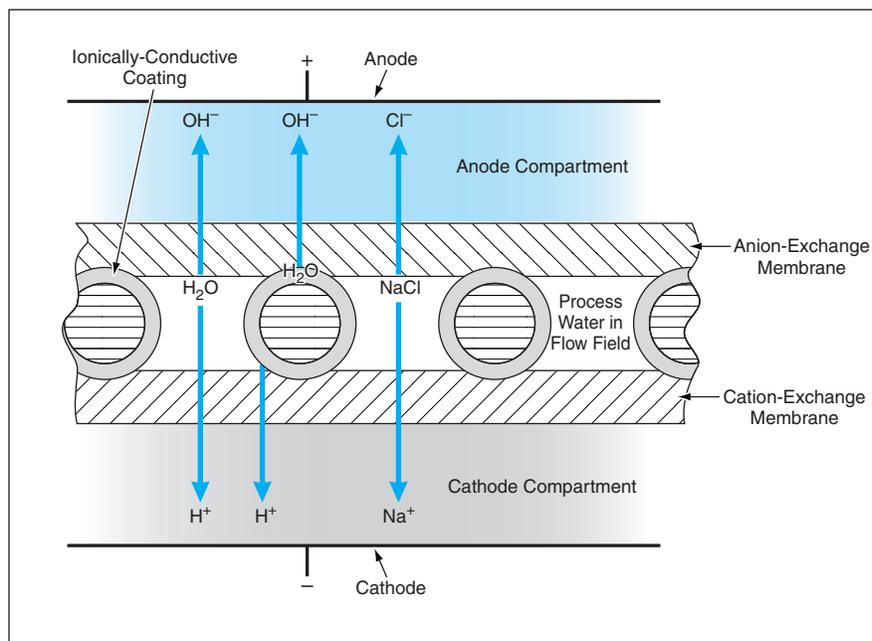
A **Bipolar Membrane Unit** contains a flow-field structure and solid electrolytes configured to provide conductive paths for the removal of ions from process water.

ionic solution. The electrodes are made of titanium coated with platinum.

The process water is introduced into the BMU, and a dc potential is applied between the electrodes. The ion-exchange membranes contain networks of molecular-size pores with electric charges fixed to their matrices. An ion-exchange membrane is nominally electronically nonconductive but is conductive to counterions; that is, to ions of charge opposite that of the ions immobilized in it. Because of the semipermeability of the membranes and the direction of the electric field between the electrodes, negatively charged ions migrate from the process water towards the anode and positively charged ions migrate from the process water towards the cathode. The ions thus removed from the process water become concentrated in the water in the anode and cathode compartments.

The removal of ions from the process water includes salt-splitting reactions (e.g., the separation of Na^+ and Cl^- ions). In addition, some water molecules dissociate into H^+ and OH^- ions. The

combination of this water splitting reaction and the highly efficient transfer of the H^+ and OH^- ions by the respective membranes ensures high transmembrane ionic conductivity, even when the concentrations of other ions in the process water are low. The ion-conducting circuit of the electrochemical cell is completed by the anode and cathode compartments.

Safer Electrolytes for Lithium-Ion Cells

John H. Glenn Research Center, Cleveland, Ohio

A number of nonvolatile, low-flammability liquid oligomers and polymers based on aliphatic organic carbonate molecular structures have been found to be suitable to be blended with ethylene carbonate to make electrolytes for lithium-ion electrochemical cells. Heretofore, such electrolytes have often been made by blending ethylene carbonate with volatile, flammable organic carbonates. The present nonvolatile electrolytes have been found to have adequate conductivity (about 2 mS/cm) for lithium ions and to remain liquid at temperatures down to –5 °C. At normal charge and discharge rates, lithium-ion cells containing these nonvolatile electrolytes but otherwise of standard design have been found to operate at current and energy densities comparable to those of cells now in common use. They do not perform well at high charge and discharge rates — an effect probably attributable to electrolyte viscosity. Cells containing the nonvolatile electrolytes have also been found to be, variously, nonflammable or at least self-extinguishing. Hence, there appears to be a basis for the development of safer high-performance lithium-ion cells.

Mechanics

⊕ Rotating Reverse-Osmosis for Water Purification
## This device would resist fouling.

Lyndon B. Johnson Space Center, Houston, Texas

A new design for a water-filtering device combines rotating filtration with reverse osmosis to create a rotating reverse-osmosis system. Rotating filtration has been used for separating plasma from whole blood, while reverse osmosis has been used in purification of water and in some chemical processes. Reverse-osmosis membranes are vulnerable to concentration polarization — a type of fouling in which the chemicals meant not to pass through the reverse-osmosis membranes accumulate very near the surfaces of the membranes. The combination of rotating filtration and reverse osmosis is intended to prevent concentration polarization and thereby increase the desired flux of filtered water while decreasing the likelihood of passage of undesired chemical species through the filter. Devices based on this concept could be useful in a variety of commercial applications, including purification and desalination of drinking water, purification of pharmaceutical process water, treatment of household and industrial wastewater, and treatment of industrial process water.

A rotating filter consists of a cylindrical porous microfilter rotating within a stationary concentric cylindrical outer shell (see figure). The aqueous suspension enters one end of the annulus between the inner and outer cylinders. Filtrate passes through the rotating cylindrical microfilter and is removed via a hollow shaft. The concentrated suspension is removed at the end of the annulus opposite the end where the suspension entered.

The effectiveness of a rotating filter in preventing fouling comes from high fluid shear caused by the rotation and from the appearance of a vortical flow structure known as Taylor vortices: the resultant flow field tends to wash particles off the rotating filter.

In reverse osmosis, water is forced at high pressure through a membrane made of a material through which contaminants in aqueous solution pass much more slowly than does water. Hence, the concentration of undesired dissolved compounds is decreased by
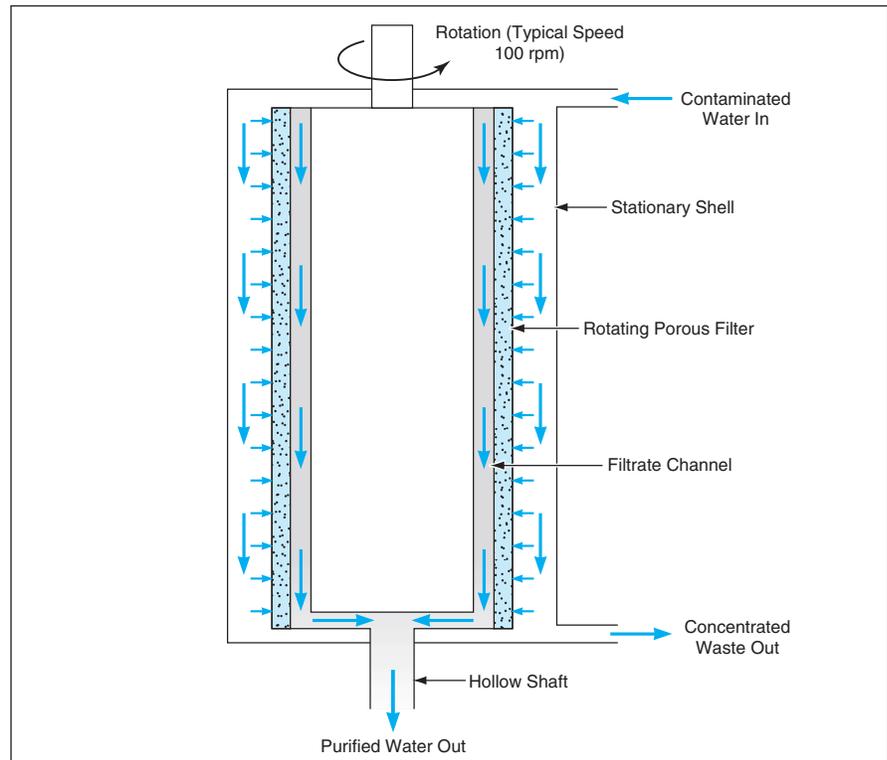
The Flow Through a Rotating Osmosis Device is shown. Shear and vortices that arise in the liquid flowing between the rotating filter and the stationary outer shell wash away material that would otherwise accumulate on or near the filter surface and thereby cause fouling.

forcing the water through the membrane, creating purified water. In conventional practice, concentration polarization of reverse-osmosis membranes is often reduced by using cross-flows (flows parallel to the membrane surfaces) to wash away the concentrated chemicals, but this is not always effective without cleaning or back washing.

The rotating reverse-osmosis device resembles a conventional rotating filter, except that the cylindrical porous microfilter is replaced with a cylindrical reverse-osmosis membrane. The shear and the Taylor vortices generated by the rotation of the cylindrical reverse-osmosis membrane wash away the concentration-polarization layer. The latest prototype of a rotating reverse-osmosis module incorporates special rotating seals to solve one of the most difficult problems in the system, enabling the device to withstand the differential pressures needed for

operation period: Whereas microfiltration systems operate at differential pressures of the order of 1 atmosphere (≈0.1 MPa), reverse-osmosis systems operate at differential pressures as high as 30 to 50 atmospheres (≈3 to 5 MPa).

Making Precise Resonators for Mesoscale Vibratory Gyroscopes

It is essential to polish wafers to precise flatness and uniform thickness.

NASA's Jet Propulsion Laboratory, Pasadena, California

An alternative approach to the design and fabrication of vibratory gyroscopes is founded on the use of fabrication techniques that yield best results in the mesoscopic size range, which is characterized by overall device dimensions of the order of a centimeter. This approach stands in contradistinction to prior approaches in (1) the macroscopic size range (the size range of conventional design and fabrication, characterized by overall device dimensions of many centimeters) and (2) the microscopic size range [the size range of microelectromechanical systems (MEMS), characterized by overall device dimensions of the order of a millimeter or less]. The mesoscale approach offers some of the advantage of the MEMS approach (sizes and power demands smaller than those of the macroscale approach) and some of the advantage of the macroscale approach (the possibility of achieving relative dimensional precision greater than that of the MEMS approach).

Relative dimensional precision is a major issue in the operation of a vibratory gyroscope. The heart of a vibratory gyroscope is a mechanical resonator that is required to have a specified symmetry in a plane orthogonal to the axis about which rotation is to be measured. If the resonator could be perfectly symmetrical, then in the absence of rotation, a free vibration of the resonator could remain fixed along any orientation relative to its housing; that is, the gyroscope could exhibit zero drift. In practice, manufacturing imprecision gives rise to some asymmetry in mass, flexural stiffness or dissipation, resulting in a slight drift or beating motion of an initial vibration pattern that cannot be distinguished from rotation.

In the mesoscale approach, one exploits the following concepts: For a given amount of dimensional error generated in manufacturing, the asymmetry and hence the rate-of-rotation drift of the gyroscope can be reduced by increasing the scale. The decrease in asymmetry also reduces coupling of vibrations to the external environment. Mechanical thermal noise and electronic measurement noise and drift can also be reduced by increasing the size of the resonator and its associated sensors.

In the mesoscale approach, a resonator is fabricated from a silicon wafer. Central to the mesoscale approach is a combination of (1) precise polishing of both faces of the wafer to form parallel planar upper and lower resonator surfaces and (2) dry reactive-ion etching (DRIE) to remove material from the sides of the resonator perpendicular to the upper and lower surfaces.

An experimental resonator was designed and fabricated following the mesoscale approach. Its frequency split (the difference between the natural frequencies of its two nominal orthogonal vibration modes — a measure of its asymmetry) was so small as to be undetectable at a resonance quality factor (Q) of 10^5, as observed in operation in a nominal vacuum with residual pressure of 10^{-5} torr ($\approx 1.3 \times 10^{-3}$ Pa). Throughout intensive experimentation, it was observed that keeping the thickness of the wafer as nearly uniform as possible was the main requirement for keeping the frequency split small, whereas the frequency split was not much affected by the side-wall roughness resulting from DRIE.

Robotic End Effectors for Hard-Rock Climbing

End effectors emulate equipment used by human climbers.

NASA's Jet Propulsion Laboratory, Pasadena, California

Special-purpose robot hands (end effectors) now under development are intended to enable robots to traverse cliffs much as human climbers do. Potential applications for robots having this capability include scientific exploration (both on Earth and other rocky bodies in space), military reconnaissance, and outdoor search and rescue operations.

Until now, enabling robots to traverse cliffs has been considered too difficult a task because of the perceived need of prohibitively sophisticated planning algorithms as well as end effectors as dexterous as human hands. The present end effectors are being designed to enable robots to attach themselves to typical rock-face features with less planning and simpler end effectors. This advance is based on the emulation of the equipment used by human climbers rather than the emulation of the human hand. Climbing-aid equipment, specifically cams, aid hooks, and cam hooks, are used by sport climbers when a quick ascent of a cliff is desired (see Figure 1).

Currently two different end-effector designs have been created. The first, denoted the simple hook emulator, consists of three "fingers" arranged around a central "palm." Each finger emulates the function of a particular type of climbing hook (aid hook, wide cam hook, and a narrow cam hook). These fingers are connected to the palm via a mechanical linkage actuated with a leadscrew/nut.

This mechanism allows the fingers to be extended or retracted. The second design, denoted the advanced hook emulator (see Figure 2), shares these features, but it incorporates an aid hook and a cam hook into each finger. The spring-loading of the aid hook allows the passive selection of the type of hook used.

The end effectors can be used in several different modes. In the aid-hook mode, the aid hook on one of the fingers locks onto a horizontal ledge while the other two fingers act to stabilize the end effector against the cliff face. In the cam-hook mode, the broad, flat tip of the cam hook is inserted into a non-horizontal crack in the cliff face. A subsequent transfer of weight onto the end ef-

BASIC HOOK
Hooks Onto Flats or Over Lips

CAM HOOK
Self Locking Cam
Between Walls of a Crack

CAM
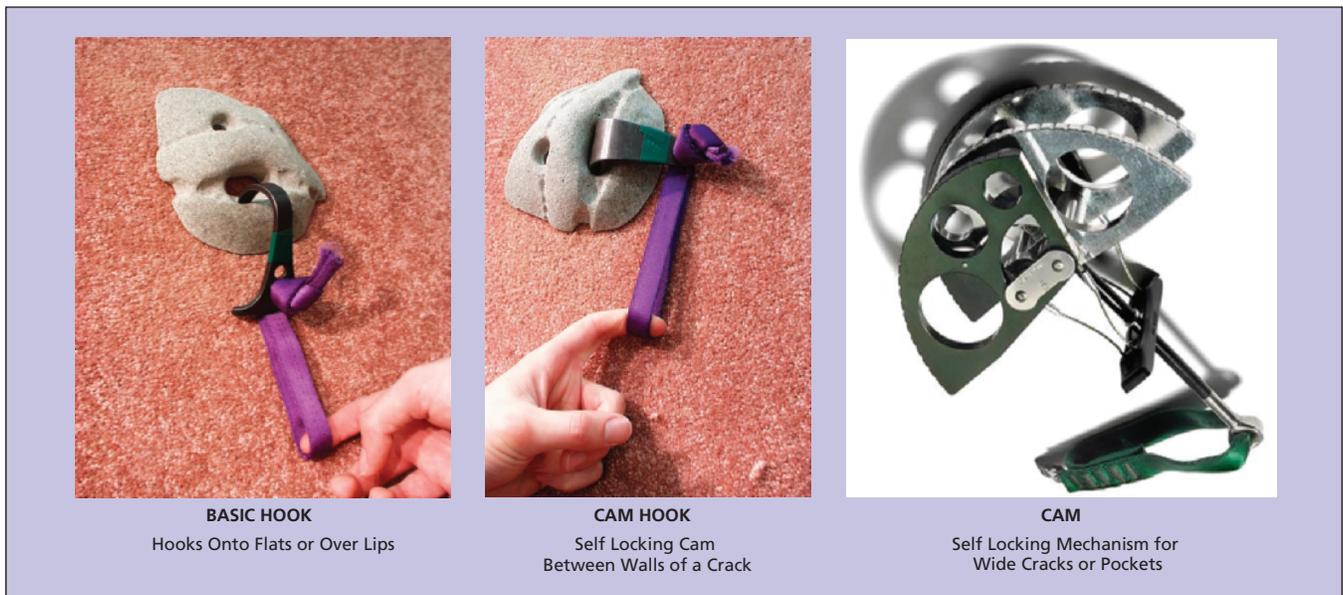Self Locking Mechanism for
Wide Cracks or Pockets

Figure 1. **Equipment Now Used by Human Rock Climbers** includes specially designed hooks, cams, and hook-and-cam assemblies. Elements of these items are being incorporated into robotic end effectors for rock climbing.

AID HOOK IN ACTION

CAM HOOK IN ACTION

Figure 2. The **Advanced Hook Emulator** can function in a variety of modes. The aid-hook and cam-hook modes shown here correspond to the modes of operation of the conventional basic hook and cam hook, respectively, depicted in Figure 1.

fector causes the tip to rotate within the crack, creating a passive, self-locking action of the hook relative to the crack. In the advanced hook emulator, the aid hook is pushed into its retracted position by contact with the cliff face as the cam hook tip is inserted into the crack. When a cliff face contains relatively large pockets or cracks, another type of passive self-locking can be used. Emulating the function of the piece of climbing equipment called a "cam" (note: not the same as a "cam hook"; see Figure 1), the fingers can be fully retracted and the entire end effector inserted into the feature. The fingers are then extended as far as the feature allows. Any weight then transferred to the end effector will tend to extend the fingers further due to frictional force, passively increasing the grip on the feature. In addition to the climbing modes, these end effectors can be used to walk on (either on the palm or the fingertips) and to grasp objects by fully extending the fingers.

This work was done by Brett Kennedy and Patrick Leger of Caltech for **NASA's Jet Propulsion Laboratory**. *Further information is contained in a TSP (see page 1).*
NPO-40224

Improved Nutation Damper for a Spin-Stabilized Spacecraft

Goddard Space Flight Center, Greenbelt, Maryland

A document proposes an improved liquid-ring nutation damper for a spin-stabilized spacecraft. The improvement addresses the problem of accommodating thermal expansion of the damping liquid. Heretofore, the problem has been solved by either (1) filling the ring completely with liquid and accommodating expansion by attaching a bellows or (2) partially filling the ring and accepting the formation of bubbles. The disadvantage of (1) is that a bellows is expensive and may not be reliable; the disadvantage of (2) is that bubbles can cause fluid lockup and consequent loss of damping. In the improved damper, the ring would be nearly completely filled with liquid, and expansion would be accommodated, but not by a bellows. Instead, an escape tube would be attached to the ring. The escape tube would be positioned and oriented so that the artificial gravitation and the associated buoyant force generated by the spin of the spacecraft would cause the bubbles to migrate toward the tip of the tube. In addition, when the spacecraft was on the launch pad, the escape tube would be at the top of the ring, so that bubbles would rise into the tube.

This work was done by Mark A. Woodard of **Goddard Space Flight Center**. *Further information is contained in a TSP (see page 1).*
GSC-14733-1

Exhaust Nozzle for a Multitube Detonative Combustion Engine

Pressures at outlets of combustor tubes are approximately constant.

Marshall Space Flight Center, Alabama

An improved type of exhaust nozzle has been invented to help optimize the performances of multitube detonative combustion engines. The invention is applicable to both air-breathing and rocket engines used to propel some aircraft and spacecraft, respectively.

In a detonative combustion engine, thrust is generated through the expulsion of combustion products from a detonation process in which combustion takes place in a reaction zone coupled to a shock wave. The combustion releases energy to sustain the shock wave, while the shock wave enhances the combus-

tion in the reaction zone. The coupled shockwave/reaction zone, commonly referred to as a detonation, propagates through the reactants at very high speed — typically of the order of several thousands of feet per second (of the order of 1 km/s). The very high speed of the detonation forces combustion to occur very rapidly, thereby contributing to high thermodynamic efficiency.

A detonative combustion engine of the type to which the present invention applies includes multiple parallel cylindrical combustion tubes, each closed at the front end and open at the rear end. Each

tube is filled with a fuel/oxidizer mixture, and then a detonation wave is initiated at the closed end. The wave propagates rapidly through the fuel/oxidizer mixture, producing very high pressure due to the rapid combustion. The high pressure acting on the closed end of the tube contributes to forward thrust. When the detonation wave reaches the open end of the tube, it produces a blast wave, behind which the high-pressure combustion products are expelled from the tube.

The process of filling each combustion tube with a detonable fuel/oxidizer mixture and then producing a detonation is
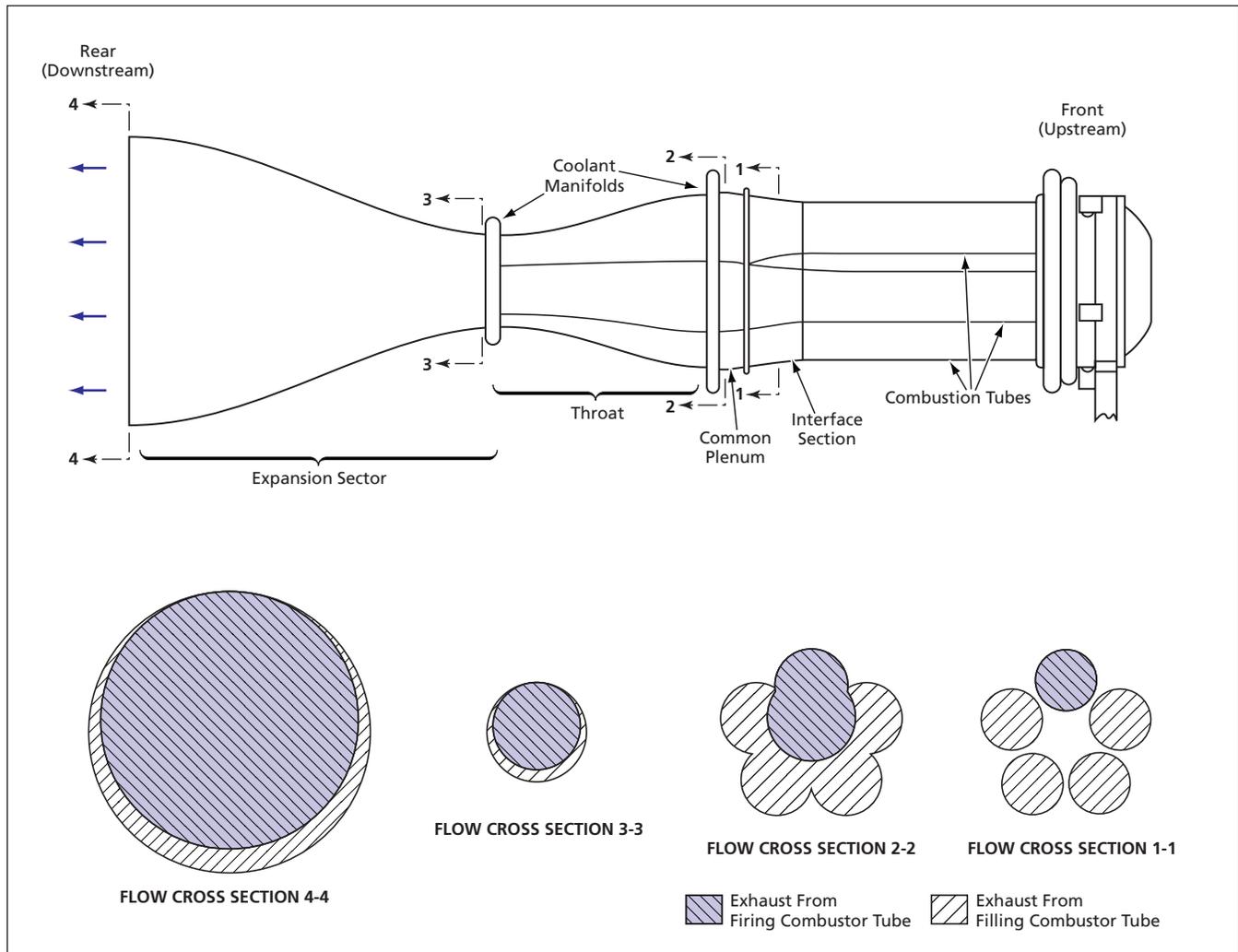
Sequentially Pulsed Exhaust Streams from multiple combustion tubes are channeled in such a manner as to maintain a nearly steady back pressure needed for refilling the combustion tubes with fuel/oxidizer mixture.

repeated rapidly to obtain repeated pulses of thrust. Moreover, the multiple combustion tubes are filled and fired in a repeating sequence. Hence, the pressure at the outlet of each combustion tube varies cyclically. A nozzle of the present invention channels the expansion of the pulsed combustion gases from the multiple combustion tubes into a common exhaust stream, in such a manner as to enhance performance in two ways:

(1) It reduces the cyclic variations of pressure at the outlets of the combustion tubes so as to keep the pressure approximately constant near the optimum level needed for filling the tubes, regardless of atmospheric pressure at the altitude of operation; and

(2) It maximizes the transfer of momentum from the exhaust gas to the engine, thereby maximizing thrust.

The figure depicts a typical engine equipped with a nozzle according to the invention. The nozzle includes an interface section comprising multiple intake ports that couple the outlets of the combustion tubes to a common plenum. Proceeding from its upstream to its downstream end, the interface section tapers to a larger cross-sectional area for flow. This taper fosters expansion of the exhaust gases flowing from the outlets of the combustion tubes and contributes to the desired equalization of exhaust combustion pressure.

The cross-sectional area for flow in the common plenum is greater than, or at least equal to, the combined cross-sectional flow areas of the combustor tubes. In the common plenum, the exhaust streams from the individual combustion tubes mix to form a single compound subsonic exhaust stream. Downstream of the common plenum is the throat that tapers to a smaller flow cross section. In this throat, the exhaust gases become compressed to form a compound sonic gas stream.

Downstream of the throat is an expansion section, which typically has a bell or a conical shape. (The expansion section can be truncated or even eliminated in the case of an air-breathing engine.) After entering the expansion section, the exhaust gases expand rapidly from compound sonic to compound supersonic speeds and are then vented to the environment.

The basic invention admits of numerous variations. For example, the combustion tubes can be arranged around the central axis in a symmetrical or asymmetrical pattern other than the one shown in the figure. For another example, the flow cross-sectional area(s) of one or more of the intake ports in the interface section, of the common plenum, the throat, and/or the expansion section can be varied, either symmetrically or asymmetrically, to adjust dynamics of the exhaust stream or to direct the thrust vector away from the central axis.

This work was done by Thomas E. Bratkovich, Kevin E. Williams, Thomas R. A. Bussing, Gary L. Lidstone, and John B. Hinkey of Adroit Systems, Inc., for **Marshall Space Flight Center**. *Further information is contained in a TSP (see page 1).*
MFS-32032

✿ Arc-Second Pointer for Balloon-Borne Astronomical Instrument

A notable innovation would eliminate effects of static friction in bearings.

Goddard Space Flight Center, Greenbelt, Maryland

A control system has been designed to keep a balloon-borne scientific instrument pointed toward a celestial object within an angular error of the order of an arc second. The design is intended to be adaptable to a large range of instrument payloads. The initial payload to which the design nominally applies is considered to be a telescope, modeled as a simple thin-walled cylinder 24 ft (≈7.3 m) long, 3 ft (≈0.91 m) in diameter, weighing 1,500 lb (having a mass of ≈680 kg).

The instrument would be mounted on a set of motor-driven gimbals in pitch-yaw configuration. The motors on the gimbals would apply the control torques needed for fine adjustments of the instrument in pitch and yaw. The pitch-yaw mount would, in turn, be suspended from a motor mount at the lower end of a pair of cables hanging down from the balloon (see figure). The motor in this mount would be used to effect coarse azimuth control of the pitch-yaw mount.

A notable innovation incorporated in the design is a provision for keeping the gimbal bearings in constant motion. This innovation would eliminate the deleterious effects of static friction — something that must be done in order to achieve the desired arc-second precision.

Another notable innovation is the use of linear accelerometers to provide feedback that would facilitate the early detection and counteraction of disturbance torques before they could integrate into significant angular-velocity and angular-position errors. The control software processing the sensor data
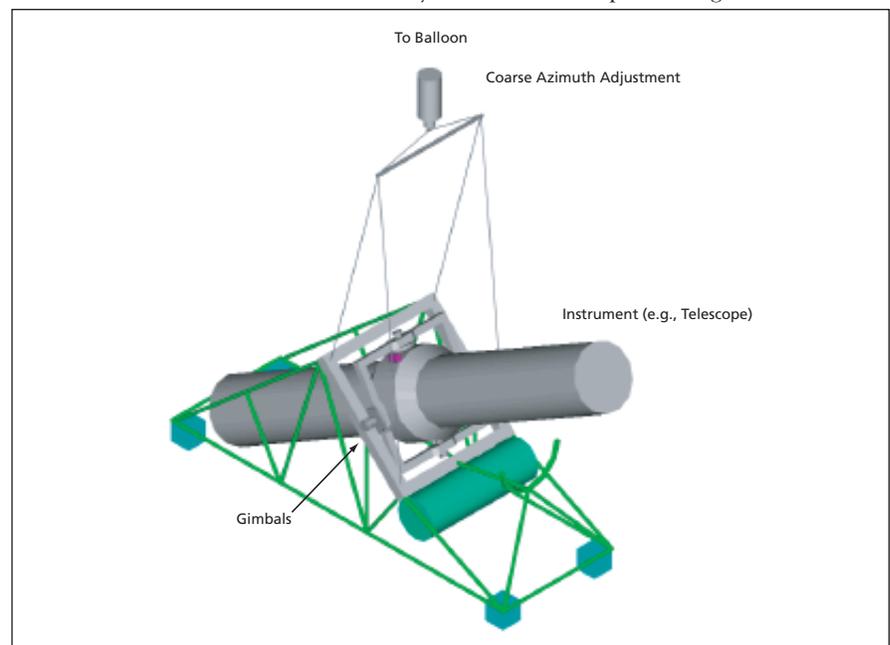
An **Instrument Would Be Suspended** below a balloon on motor-driven gimbals at the lower end of a set of cables. The motors would apply torques to correct pointing errors.

would be capable of distinguishing between translational and rotational accelerations. The output of the accelerometers is combined with that of angular position and angular-velocity sensors into a proportional + integral + derivative + acceleration control law

for the pitch and yaw torque motors. Preliminary calculations have shown that with appropriate gains, the power demand of the control system would be low enough to be satisfiable by means of storage batteries charged by solar batteries during the day.

✿ Compact, Automated Centrifugal Slide-Staining System

Small quantities of different liquids would be displaced at different centrifuge speeds.

Lyndon B. Johnson Space Center, Houston, Texas

The Directional Acceleration Vector-Driven Displacement of Fluids (DAVD-DOF) system, under development at the time of reporting the information for this article, would be a relatively compact, automated, centrifugally actuated system for staining blood smears and other microbiological samples on glass microscope slides in either a microgravitational or a normal Earth gravitational environment. The DAVD-DOF concept is a successor to the centrifuge-operated slide stainer (COSS) concept, which was reported in "Slide-Staining System for Microgravity or Gravity" (MSC-22949), *NASA Tech Briefs,* Vol. 25, No. 1 (January, 2001), page 64. The COSS includes reservoirs and a staining chamber that contains a microscope slide to which a biological sample is affixed. The staining chamber is sequentially filled with and drained of staining and related liquids from the reservoirs by use of a weighted plunger to force liquid from one reservoir to another at a constant level of hypergravity maintained in a standard swing-bucket centrifuge.

In the DAVD-DOF system, a staining chamber containing a sample would also be sequentially filled and emptied, but with important differences. Instead of a simple microscope slide, one would use a special microscope slide on which would be fabricated a network of very small reservoirs and narrow channels connected to a staining chamber (see figure). Unlike in the COSS, displacement of liquid would be effected by use of the weight of the liquid itself, rather than the weight of a plunger.

The channel from each reservoir to the staining chamber would be made so narrow that the combination of surface tension of the liquid and friction between the liquid and the channel surface would suffice to prevent the flow of liquid from the reservoir to the staining chamber in the absence of hypergravitational centrifugal acceleration below

a specified level. Downstream of the staining chamber, there would be channel for draining each fluid from the staining chamber into a waste reservoir after use; this channel would be wider than the other channels so that draining could be accomplished at a centrifuge speed much lower than that needed for filling the staining chamber from a reservoir. Flow in this channel would be restricted by an electrically actuated microvalve controlled by a microprocessor on the spindle of the centrifuge.

By suitable choice of width of each channel, taking account of properties and amount of each liquid, the threshold centrifugal accelerations for moving the liquids from the reservoirs to the staining chamber would be set at successively
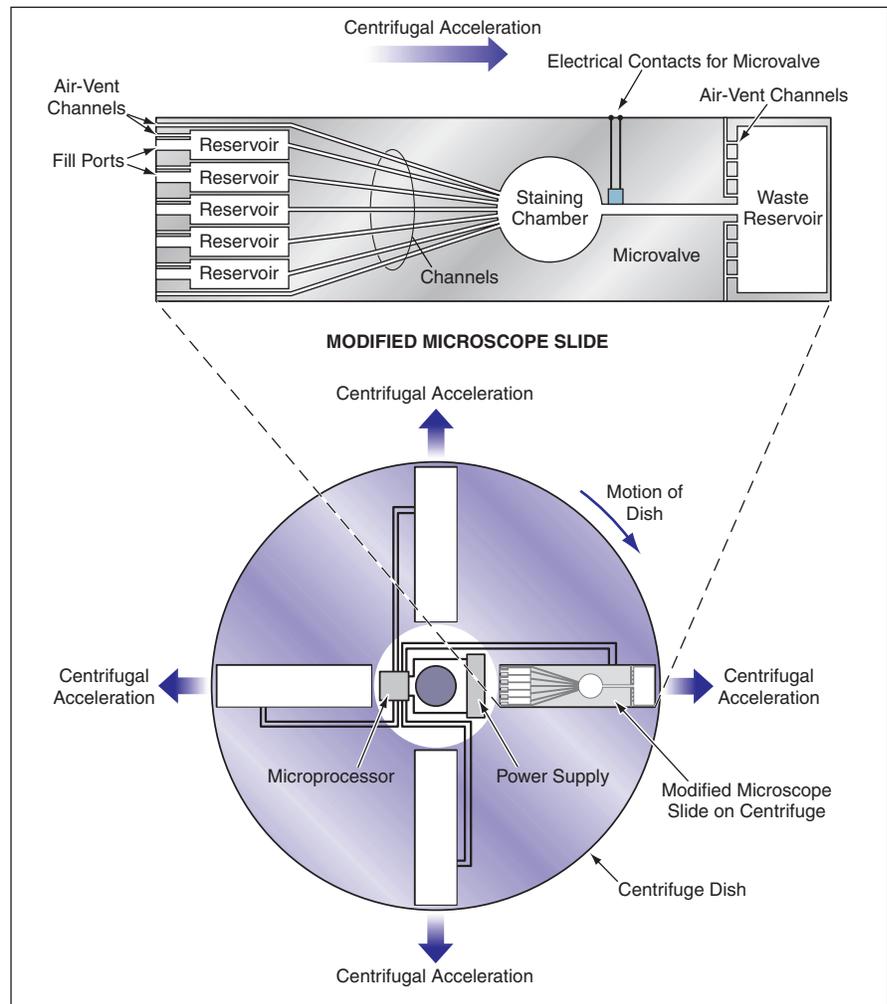
Liquids Would Be Contained in Small Reservoirs on a modified microscope slide. Different liquids would be transferred into the staining chamber at different centrifuge speeds.

greater values in the sequence in which the liquids were required to be used. Then sequential filling of the staining chamber with the various liquids would be achieved by momentarily increasing the speed of the centrifuge to exceed the corresponding threshold accelerations at the required times. Once the sample had been exposed to each liquid for the required time, the valve would be opened to drain the liquid from the staining chamber into the waste reservoir.

The reservoirs, channels, and staining chamber could be created, either on a glass slide or on a uniformly thick coating material on the slide, by one or more of a variety of techniques that could involve photolithography, laser writing, and/or etching. Once a slide had been thus prepared, a sample would be placed on the staining-chamber area of a thin glass cover, then cover would be adhesively or electrostatically bonded to the slide or to the coating material. The liquids would then be dispensed into their assigned reservoirs via access ports and the air displaced from the reservoirs would leave through vent ports. The slide would then be placed on a centrifuge in the form of a spinning disk, and the centrifuge would be operated as described above to expose the sample sequentially to the various liquids.

Two-Armed, Mobile, Sensate Research Robot

This could be a prototype of robotic home health-care aides.

Lyndon B. Johnson Space Center, Houston, Texas

The Anthropomorphic Robotic Testbed (ART) is an experimental prototype of a partly anthropomorphic, humanoid-size, mobile robot. The basic ART design concept provides for a combination of two-armed coordination, tactility, stereoscopic vision, mobility with navigation and avoidance of obstacles, and natural-language communication, so that the ART could emulate humans in many activities. The ART could be developed into a variety of highly capable robotic assistants for general or specific applications. There is especially great potential for the development of ART-based robots as substitutes for live-in health-care aides for home-bound persons who are aged, infirm, or physically handicapped; these robots could greatly reduce the cost of home health care and extend the term of independent living.

The ART is a fully autonomous and untethered system. It includes a mobile base on which is mounted an extensible torso topped by a head, shoulders, and two arms. All subsystems of the ART are powered by a rechargeable, removable battery pack. The mobile base is a differentially-driven, nonholonomic vehicle capable of a speed >1 m/s and can handle a payload >100 kg. The base can be controlled manually, in forward/backward and/or simultaneous rotational motion, by use of a joystick. Alternatively, the motion of the base can be controlled autonomously by an onboard navigational computer.

By retraction or extension of the torso, the head height of the ART can be adjusted from 5 ft (1.5 m) to 6 1/2 ft (2 m), so that the arms can reach either the floor or high shelves, or some ceilings. The arms are symmetrical. Each arm (including the wrist) has a total of six rotary axes like those of the human shoulder, elbow, and wrist joints. The arms are actuated by electric motors in combination with brakes and gas-spring assists on the shoulder and elbow joints. The arms are operated under closed-loop digital control. A receptacle for an end effector is mounted on the tip of the wrist and contains a force-and-torque sensor that provides feedback for force (compliance) control of the arm. The end effector could be a tool or a robot hand, depending on the application.

The ART includes several built-in, ready-to-use sensory subsystems and has room for addition of other sensors. One of the built-in sensory subsystems is a bumper/shield subsystem that includes mechanical tape switches and photodetectors to detect actual or incipient collisions with objects on the floor, plus ultrasonic sensors to detect nearby overhanging objects or walls. Other built-in sensory subsystems include laser-based distance measuring equipment, dual cameras for vision (including stereoscopic vision), the aforementioned force-and-torque sensors, and shaft-angle encoders and switches that provide position feedback for control of the arms. The two cameras can be panned and tilted independently of each other; they can be aimed in different directions or the same direction.

Each of the various sensory and motion-control subsystems operates in conjunction with a computer subsystem that processes the incoming sensory data and controls the affected component of the motion. The navigational computer communicates with the sensory and base-motion-control computers. Another computer processes the digitized outputs of the cameras and controls the aiming, focus, and zoom of the cameras. Still another computer processes the digitized outputs of the force-and-torque sensors and executes software for control of the motions of, and forces exerted by, the arms.

Overall control is exerted by a host computer, which is of a Pentium-based laptop class. This computer runs speech-recognition and speech-synthesis software for communication with a human user. For purposes of experimentation and development, the host computer is also capable of radio communication with an external computer or network of computers.

Compensating for Effects of Humidity on Electronic Noses

Corrections are derived from outputs of separate humidity and temperature sensors.

NASA's Jet Propulsion Laboratory, Pasadena, California

A method of compensating for the effects of humidity on the readouts of electronic noses has been devised and tested. The method is especially appropriate for use in environments in which humidity is not or cannot be controlled — for example, in the vicinity of a chemical spill, which can be accompanied by large local changes in humidity.

Heretofore, it has been common practice to treat water vapor as merely another analyte, the concentration of which is determined, along with that of the other analytes, in a computational process based on deconvolution. This practice works well, but leaves room for improvement: changes in humidity can give rise to large changes in electronic-nose responses. If corrections for humidity are not made, the large humidity-induced responses may swamp smaller responses associated with low concentrations of analytes.

The present method offers an improvement. The underlying concept is simple: One augments an electronic nose with a separate humidity and a separate temperature sensor. The outputs of the humidity and temperature sensors are used to generate values that are subtracted from the readings of the other sensors in an electronic nose to correct for the temperature-dependent contributions of humidity to those readings. Hence, in principle, what remains after corrections are the contributions of the analytes only. Laboratory experiments on a first-generation electronic nose have shown that this method is effective and improves the success rate of identification of analyte/water mixtures. Work on a second-generation device was in progress at the time of reporting the information for this article.

Brush/Fin Thermal Interfaces

High thermal conductance sliding interfaces can be achieved.

Lyndon B. Johnson Space Center, Houston, Texas

Brush/fin thermal interfaces are being developed to increase heat-transfer efficiency and thereby enhance the thermal management of orbital replaceable units (ORUs) of electronic and other equipment aboard the International Space Station. Brush/fin thermal interfaces could also be used to increase heat-transfer efficiency in terrestrial electronic and power systems.

In a typical application according to conventional practice, a replaceable heat-generating unit includes a mounting surface with black-anodized metal fins that mesh with the matching fins of a heat sink or radiator on which the unit is mounted. The fins do not contact each other, but transfer heat via radiation exchange. A brush/fin interface also includes intermeshing fins, the difference being that the gaps between the fins are filled with brushes made of carbon or other fibers. The fibers span the gap between intermeshed fins, allowing heat transfer by conduction through the fibers. The fibers are attached to the metal surfaces as velvetlike coats in the manner of the carbon-fiber brush heat exchangers described in the preceding article. The fiber brushes provide both mechanical compliance and thermal contact, thereby ensuring low contact thermal resistance.

A certain amount of force is required to intermesh the fins due to sliding friction of the brush's fiber tips against the fins. This force increases linearly with penetration distance, reaching ~1 psi (~6.9 kPa) for full 2-in. (5.1 cm) penetration for the conventional radiant fin interface. Removal forces can be greater due to fiber buckling upon reversing the sliding direction. This buckling force can be greatly reduced by biasing the fibers at an angle perpendicularly to the sliding direction. Means of containing potentially harmful carbon fiber debris, which is electrically conductive, have been developed.

Small prototype brush/fin thermal interfaces have been tested and found to exhibit temperature drops about one-sixth of that of conventional meshing-fin thermal interface, when fabricated as a retrofit. In this case, conduction through the long, thin metal fins themselves becomes a thermal bottleneck. Further improvement could be made by prescribing aluminum fins to be shorter and thicker than those of the conventional meshing-fin thermal interfaces; the choice of height and thickness would be optimized to obtain greater overall thermal conductance, lower weight, and lower cost.

Multispectral Scanner for Monitoring Plants

John F. Kennedy Space Center, Florida

A multispectral scanner has been adapted to capture spectral images of living plants under various types of illumination for purposes of monitoring the health of, or monitoring the transfer of genes into, the plants. In a health-monitoring application, the plants are illuminated with full-spectrum visible and near infrared light and the scanner is used to acquire a reflected-light spectral signature known to be indicative of the health of the plants. In a gene-transfer-monitoring application, the plants are illuminated with blue or ultraviolet light and the scanner is used to capture fluorescence images from a green fluorescent protein (GFP) that is expressed as result of the gene transfer. The choice of wavelength of the illumination and the wavelength of the fluorescence to be monitored depends on the specific GFP.

# ▶ Coding for Communication Channels With Dead-Time Constraints

Novel coding schemes may offer significant advantages in some applications.

NASA's Jet Propulsion Laboratory, Pasadena, California

Coding schemes have been designed and investigated specifically for optical and electronic data-communication channels in which information is conveyed via pulse-position modulation (PPM) subject to dead-time constraints. These schemes involve the use of error-correcting codes concatenated with codes denoted constrained codes. These codes are decoded using an interactive method.

In pulse-position modulation, time is partitioned into frames of M slots of equal duration. Each frame contains one pulsed slot (all others are non-pulsed). For a given channel, the dead-time constraints are defined as a maximum and a minimum on the allowable time between pulses. For example, if a Q-switched laser is used to transmit the pulses, then the minimum allowable dead time is the time needed to recharge the laser for the next pulse. In the case of bits recorded on a magnetic medium, the minimum allowable time between pulses depends on the recording/playback speed and the minimum distance between pulses needed to prevent interference between adjacent bits during readout. The maximum allowable dead time for a given channel is the maximum time for which it is possible to satisfy the requirement to synchronize slots. In mathematical shorthand, the dead-time constraints for a given channel are represented by the pair of integers (d,k), where d is the minimum allowable number of zeroes between ones and k is the maximum allowable number of zeroes between ones.

A system of the type to which the present schemes apply is represented by a bi-
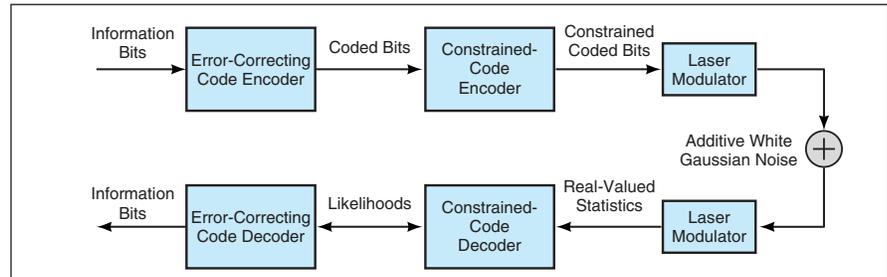
Error-Correcting and Constrained PPM Codes are concatenated at the transmitting end of a communication channel.

nary-input, real-valued-output channel model illustrated in the figure. At the transmitting end, information bits are first encoded by use of an error-correcting code, then further encoded by use of a constrained code. Several constrained codes for channels subject to constraints of (d,∞) have been investigated theoretically and computationally. The baseline codes chosen for purposes of comparison were simple PPM codes characterized by M-slot PPM frames separated by d-slot dead times.

Another category of codes investigated was that of synchronous truncated pulse-position modulation (STPPM), which is generated by implementing synchronous variable-length PPM codes in a new way. In a synchronous variable-length PPM code, mp bits are mapped to mq bits, where m, p, and q are positive integers, p and q are fixed, and m is allowed to vary. Such a code is characterized by, among other things, a rate (average number of bits per slot) of p/q. In generating a STPPM code, a procedure based partly on a binary tree is followed in mapping un-

constrained binary sequences into the applicable constraint. In addition to the dead-time constraint, the code words involved in the mapping are subject to some mathematical constraints, a description of which would greatly exceed the space available for this article.

The advantages and disadvantages of the schemes investigated are not subject to any single, simple characterization. In general, it was found that for constrained PPM codes concatenated with error-correcting codes at the transmitting end and iterative decoding at the receiving end, there are advantages over baseline schemes with respect to error rate at a given signal-to-noise ratio, throughput at a given error rate, and complexity relative to prior schemes that include iterative decoding.

This work was done by Bruce Moision and Jon Hamkins of Caltech for **NASA's Jet Propulsion Laboratory**. *Further information is contained in a TSP (see page 1).*

This software is available for commercial licensing. Please contact Don Hart of the California Institute of Technology at (818) 393-3425. Refer to NPO-30524.

▶ System for Better Spacing of Airplanes En Route

Deviations from preferred trajectories can be reduced.

Ames Research Center, Moffett Field, California

An improved method of computing the spacing of airplanes en route, and software to implement the method, have been invented. The purpose of the invention is to help air-traffic controllers minimize those deviations of the airplanes from the trajectories preferred by their pilots that are needed to make the airplanes comply with miles-in-trail spacing requirements (defined below). The software is meant to be a modular component of the Center-

TRACON Automation System (CTAS) (TRACON signifies "terminal radar approach control"). The invention reduces controllers' workloads and reduces fuel consumption by reducing the number of corrective clearances needed to achieve conformance with specified flow rates, without causing conflicts, while providing for more efficient distribution of spacing workload upstream and across air-traffic-control sectors.

Prerequisite to a meaningful summary of the invention are definitions of the terms "miles in trail" and "conflict probe":

• "Miles in trail" signifies a specified distance, in nautical miles, required to be maintained between airplanes.

• A conflict probe is a computer program that assists air-traffic controllers in maintaining safe distances between aircraft by predicting conflicts (essentially, close approaches with potential for collision) as long as 20 minutes in advance. The predictions are made by use of a combination of (1) information on the present state of the aircraft (horizontal positions, altitudes, and velocities) obtained by tracking; (2) information on the anticipated states of the aircraft obtained from flight plans; (3) information on atmospheric conditions; and (4) information on the aerodynamics and engine performance characterization of the airplanes.

In broad terms, the inventive method involves establishment of a spacing reference geometry (described below); prediction of locations of all aircraft of interest at the predicted time of intersection of the path of whichever of the aircraft is expected to first intersect the spacing reference geometry; and determination of the distances between aircraft on the basis of their predicted locations at that time. The design spacing reference geometry includes a collection of fixed waypoints (including locations of navaids, airway intersections, and predetermined latitude/longitude positions); airspace sector boundaries; arcs defined in reference to airports or other geographical locations; arbitrary lines in space; and combinations of line segments.

The software generates a display that includes the predicted locations and spacings of the aircraft of interest. The spacings can be indicated in any of a variety of formats — for example, alphanumerically on a list adjacent to a radar display showing flightpaths and spacing-reference-geometry features of a region of interest. When an alteration in flight characteristics (course, speed, and/or altitude) of one or more of the aircraft is proposed, the predicted locations and spacings are recalculated, thereby providing feedback as to conformance of the proposed alteration with the spacing requirement. In addition, a conflict probe is preferably used to determine whether the proposed alteration could cause a conflict.

By selection of spacing-calculation parameters, an air-traffic controller can specify whether the determination of spacing is one of rolling spacing, fixed spacing, absolute spacing distance, or relative spacing distance. It is possible to impose a "meet spacing" requirement, in response to which the software proposes, to the controller, changes of course, speed, and altitude of one or more of aircraft that would satisfy the spacing requirement. Aircraft may be selected by matching aircraft to input stream characteristics, as well as by directly identifying flights by controller input, and the selection process can be repeated at intervals. Spacing advisory data are preferably reported to other controllers responsible for monitoring each aircraft.

This work was done by Steven Green and Heinz Erzberger of **Ames Research Center**. *Further information is contained in a TSP (see page 1).*

This invention has been patented by NASA (U.S. Patent No. 6,393,358). Inquiries concerning nonexclusive or exclusive license for its commercial development should be addressed to the Patent Counsel, Ames Research Center, (650) 604-5104. Refer to ARC-14418.

Σ Algorithm for Training a Recurrent Multilayer Perceptron

Lyndon B. Johnson Space Center, Houston, Texas

An improved algorithm has been devised for training a recurrent multilayer perceptron (RMLP) for optimal performance in predicting the behavior of a complex, dynamic, and noisy system multiple time steps into the future. [An RMLP is a computational neural network with self-feedback and cross-talk (both delayed by one time step) among neurons in hidden layers]. Like other neural-network-training algorithms, this algorithm adjusts network biases and synaptic-connection weights according to a gradient-descent rule. The distinguishing feature of this algorithm is a combination of global feedback (the use of predictions as well as the current output value in computing the gradient at each time step) and recursiveness. The recursive aspect of the algorithm lies in the inclusion of the gradient of predictions at each time step with respect to the predictions at the preceding time step; this recursion enables the RMLP to learn the dynamics. It has been conjectured that carrying the recursion to even earlier time steps would enable

the RMLP to represent a noisier, more-complex system.

This work was done by Alexander G. Parlos, Omar T. Rais, and Sunil K. Menon of Texas A&M University and Amir F. Atiya of Caltech for **Johnson Space Center**. *For further information, contact:*

Dr. Alexander G. Parlos
Dept. of Nuclear Engineering
Texas A&M University
College Station, TX 77843
Telephone No.: (409) 845-7092,
Fax No.: (409) 845-6443
Refer to MSC-22893.

Books & Reports

Orbiter Interface Unit and Early Communication System

A report describes the Orbiter Interface Unit (OIU) and the Early Communication System (ECOMM), which are systems of electronic hardware and software that serve as the primary communication links for the International Space Station (ISS). When a space shuttle is at or near the ISS during assembly and resupply missions, the OIU sends ground- or crew-initiated commands from the space shuttle to the ISS and relays telemetry from the ISS to the space shuttle's payload data systems. The shuttle then forwards the telemetry to the ground. In the absence of a space shuttle, the ECOMM handles communications between the ISS and Johnson Space Center via the Tracking and Data Relay Satellite System (TDRSS). Innovative features described in the report include (1) a "smart" data-buffering algorithm that helps to preserve synchronization (and thereby minimize loss) of telemetric data between the OIU and the space-shuttle payload data interleaver; (2) an ECOMM antenna-autotracking algorithm that selects whichever of two phased-array antennas gives the best TDRSS signal and electronically steers that antenna to track the TDRSS source; and (3) an ECOMM radiation-latchup controller, which detects an abrupt increase in current indicative of radiation-induced latchup and temporarily turns off power to clear the latchup, restoring power after the charge dissipates.

This work was done by Ronald M. Cobbs, Michael P. Cooke, Gary L. Cox, Richard Ellenberger, Patrick W. Fink, Dena S. Haynes, Buddy Hyams, Robert Y. Ling, Helen M. Neighbors, Chau T. Phan, Kelly M. Prender-gast, James D. Siekierski, Randall S. Wade, George A. Weisskopf, Hester J. Yim, Antha A. Adkins, James R. Carl, Y. C. Loh, Charles Roberts, Douglas J. Steel, Buveneka Kan-ishka DeSilva, Harold B. Killenb, and Robert M. Williams of **Johnson Space Center**. *For further information, contact the Johnson Commercial Technology Office at (281) 483-3809.*
MSC-23225

White-Light Nulling Interferometers for Detecting Planets

A report proposes the development of a white-light nulling interferometer to be used in conjunction with a single-aperture astronomical telescope that would be operated in outer space. When such a telescope is aimed at a given star, the interferometer would suppress the light of that star while passing enough light from planets (if any) orbiting the star, to enable imaging or spectroscopic examination of the planets. In a nulling interferometer, according to the proposal, scattered light would be suppressed by spatial filtering in an array of single-mode optical fibers rather than by requiring optical surfaces to be accurate within 1/4,000 wavelength as in a coronagraph or an apodized telescope. As a result, angstrom-level precision would be needed in only the small nulling combiner, and not in large, meter-sized optics. The nulling interferometer could work as an independent instrument in space or in conjunction with a coronagraphic system to detect planets outside our solar system.

This work was done by Bertrand Mennesson, Eugene Serabyn, Michael Shao, and Bruce Levine of Caltech for **NASA's Jet Propulsion Laboratory**. *Further information is contained in a TSP (see page 1).*
NPO-30547

Development of Methodology for Programming Autonomous Agents

A brief report discusses the rationale for, and the development of, a methodology for generating computer code for autonomous-agent-based systems. The methodology is characterized as enabling an increase in the reusability of the generated code among and within such systems, thereby making it possible to reduce the time and cost of development of the systems. The methodology is also characterized as enabling reduction of the incidence of those software errors that are attributable to the human failure to anticipate distributed behaviors caused by the software. A major conceptual problem said to be addressed in the development of the methodology was that of how to efficiently describe the interfaces between several layers of agent composition by use of a language that is both familiar to engineers and descriptive enough to describe such interfaces unambivalently.

This work was done by Kutluhan Erol, Renato Levy, and Jun Lang of Intelligent Automation, Inc., for **Johnson Space Center**.
For further information, contact:
Intelligent Automation, Inc.
7519 Standish Place, (S. 200)
Rockville, MD 20855
Phone: (301) 294-5200
Fax: (301) 294-5201
E-mail: edtech@I-a-i.com
Refer to MSC-23385.

National Aeronautics and
Space Administration